TRIBHUVAN UNIVERSITY

INSTITUTE OF ENGINEERING

PULCHOWK CAMPUS

Thesis no: M-114-MSMDE-2017-2026

Assessment of PV–Wind Hybrid Microgrid Size for Rural Offgrid Environment Using Evolutionary Algorithm

by

Asmit Gautam

A THESIS

SUBMITTED TO THE DEPARTMENT OF MECHANICAL AND AEROSPACE ENGINEERING

IN PARTIAL FULFILLMENT OF THE REQUIREMENTS FOR THE

DEGREE OF MASTER OF SCIENCE IN

MECHANICAL SYSTEMS DESIGN AND ENGINEERING

DEPARTMENT OF MECHANICAL AND AEROSPACE ENGINEERING

LALITPUR, NEPAL

JUNE, 2026

TRIBHUVAN UNIVERSITY
INSTITUTE OF ENGINEERING
PULCHOWK CAMPUS
DEPARTMENT OF MECHANICAL AND AEROSPACE ENGINEERING

The undersigned certify that they have read, and recommended to the Institute of Engineering for acceptance, a thesis entitled "Assessment of PV–Wind Hybrid Microgrid Size for Rural Offgrid Environment Using Evolutionary Algorithm" submitted by Asmit Gautam in partial fulfillment of the requirements for the Master in Mechanical Systems Design and Engineering.

Supervisor
Assoc. Prof. Dr. Hari Bahadur Darlami
Department of Mechanical and Aerospace Engineering
Pulchowk Campus, Institute of Engineering

External Examiner
Assoc. Prof. Dr. Shailendra Kumar Jha
Kathmandu University, Dhulikhel, Nepal

Tribhuvan University
Institute of Engineering
Department of Mechanical and Aerospace Engineering
Pulchowk Campus

Committee Chairperson,
Asst. Prof. Dr. Sudip Bhattarai
Head of Department
Department of Mechanical and Aerospace Engineering
Pulchowk Campus, Institute of Engineering

Date: 12 June, 2026

iii

Abstract

Off-grid electrification in rural isolated communities presents challenges due to rugged terrain, extreme weather, sparse settlement, socio-financial and technical challenges. This thesis develops a Python-based multi-objective optimization framework employing NSGA-II to size photovoltaic (PV)-wind-battery microgrid systems, balancing capital expenditure against reliability; measured by unmet load fraction for a baseline load of 87 kWh/day for Chisapani, Hariharpurgadhi Village, Sindhuli District, Nepal. We generate a Pareto front comprising 50 non-dominated solutions with costs from approximately USD 12,000 to USD 95,000 and unmet load fractions from 0.81 down to 0.17. Through detailed analyses of cost–reliability trade-offs, energy-mix contributions, and design-space clustering, we identify three practical design regimes PV-led, hybrid transition, and wind-storage focused mapped to specific budget bands and reliability targets. Robustness assessments, including ±10% resource variations quantify performance sensitivity and uncertainty bounds while benchmarking against HOMER-based studies demonstrates competitive Levelized Cost of Electricity and reliability outcomes. Finally, we propose phased implementation strategies, policy recommendations, and future enhancements such as integration of measured meteorological data, multi-year simulations, detailed component models, and participatory multi-criteria optimization. The open-source algorithm offers decision-makers and implementers transparent, reproducible decision support for cost-effective and resilient microgrid investments in diverse off-grid environments.

Keywords: microgrid optimization; multi-objective evolutionary algorithm; NSGA-II; photovoltaic; wind energy; battery storage; Pareto front; reliability; off-grid electrification; Rural communities; sensitivity analysis; Levelized Cost of Electricity; open-source framework

Acknowledgement

I would like to express my sincere gratitude to my supervisor, Dr. Hari Bahadur Darlami Associate Professor (Renewable Energy and Alternative Fuel) , for his invaluable guidance, constant encouragement, and inspiration. I feel honored to work under his supervision. My sincere thanks go to Dr. Sudip Bhattarai, Head, Department of Mechanical and Aerospace Engineering, Pulchowk Campus for providing the opportunity to undertake this thesis. I also thank coordinator of the MSc. Mechanical Systems Design and Engineering program, for his valuable suggestions. My appreciation extends to Ms. Yasodha Adhikari, administrator of the Department of Mechanical Engineering, IOE Pulchowk Campus, for her unwavering support.

I am deeply grateful to my colleagues and teachers for their continuous support and constructive feedback. I am highly indebted to those who provided valuable suggestions at various stages of this thesis. Special thanks goes to my classmates (073 Batch, Mechanical Systems Design and Engineering) and all individuals directly or indirectly involved in this work for their kind interest and support.

Table of Contents

List of Tables

List of Figures

List of Abbreviations

AC	Alternating Current
BMS	Battery Management System
CO_2	Carbon Dioxide
DC	Direct Current
EMS	Energy Management System
GHI	Global Horizontal Irradiance
GWO	Grey Wolf Optimizer
HOMER Pro	Hybrid Optimization of Multiple Energy Resources (Pro)
LCOE	Levelized Cost of Electricity
LFP	Lithium Iron Phosphate (battery chemistry)
LOLP	Loss of Load Probability
LP / MILP	Linear Programming / Mixed-Integer Linear Programming
MC	Monte Carlo
MPPT	Maximum Power Point Tracking
NMC	Nickel Manganese Cobalt (battery chemistry)
NSGA-II	Non-Dominated Sorting Genetic Algorithm II
O&M	Operation and Maintenance
POA	Plane of Array (irradiance)
PSO	Particle Swarm Optimization
PV	Photovoltaic
SOC	State of Charge
TMY	Typical Meteorological Year

CHAPTER ONE: INTRODUCTION

1.1 Background

Access to reliable and sustainable energy is a critical challenge for remote Rural villages in Nepal, where geographical isolation, rugged terrain, and limited infrastructure hinder the extension of conventional power grids. Historically, these communities have relied on traditional energy sources such as firewood, kerosene, and diesel generators for lighting, heating, and other basic needs. However, these sources are often unsustainable, environmentally harmful, and expensive, contributing to deforestation, indoor air pollution, and high operational costs. With the global shift toward renewable energy, photovoltaic (PV) and wind-based hybrid microgrids have emerged as viable solutions for off-grid electrification in remote areas. These systems integrate solar panels, wind turbines, energy storage (e.g., batteries), and sometimes backup generators to provide a stable and sustainable power supply. The design and sizing of such hybrid microgrids require careful optimization to balance multiple objectives, including cost minimization, system reliability, and environmental sustainability.

The Rural region, characterized by abundant solar radiation and seasonal wind patterns, presents a unique opportunity for deploying PV wind hybrid microgrids. Solar energy is plentiful during clear days, while wind energy can complement power generation during cloudy or monsoon seasons, reducing dependency on a single renewable source. However, the intermittent nature of solar and wind resources introduces challenges in ensuring consistent power supply, necessitating energy storage and backup systems. Moreover, the design of microgrids must account for the non-linear and dynamic behavior of renewable energy systems, as fluctuations in solar irradiance, wind speed, and load demand can lead to system inefficiencies or failures (Shrestha et al., 2018). The sizing of microgrid components such as the number of PV panels, wind turbines, battery capacity, and generator size requires a multi-objective optimization approach to achieve an optimal balance between cost, reliability, and environmental impact.

The primary functions of a PV–wind hybrid microgrid in Rural villages are: i. To provide a reliable and continuous power supply to meet the community's energy demands.

ii. To minimize the total system cost, including capital, operational, and maintenance expenses.

iii. To reduce environmental impact by maximizing renewable energy utilization and minimizing reliance on fossil fuel-based backup systems.

These objectives are inherently interdependent, and optimizing one often comes at the expense of another. For instance, increasing battery capacity enhances reliability but raises costs, while reducing generator use lowers emissions but may compromise power availability during low renewable generation periods. The application of evolutionary algorithms enables the identification of a Pareto-optimal set of solutions, allowing decision-makers to select configurations that best align with community priorities and resource constraints (Rana & Kumar, 2019).

1.2 Components of a PV–Wind Hybrid Microgrid

The basic components of a PV–wind hybrid microgrid system are as follows:

i. Photovoltaic (PV) Panels: Convert solar energy into electrical energy, serving as the primary renewable energy source during daylight hours.
ii. Wind Turbines: Generate electricity from wind energy, complementing PV panels during periods of low solar availability, such as cloudy or windy seasons.
iii. Battery Storage: Stores excess energy generated by PV panels and wind turbines to ensure a continuous power supply during periods of low generation.
iv. Backup Generator: Typically diesel-based, provides supplementary power during extended periods of insufficient renewable energy generation.
v. Inverter: Converts direct current (DC) from PV panels and batteries to alternating current (AC) for use in household and community appliances.
vi. Control System: Manages the operation of microgrid components, ensuring efficient energy flow and system stability.

1.3 Problem Statement

Rural villages remain on the fringes of electrification narrative, with over 40% of households lacking dependable access to electricity due to formidable terrain, extreme climatic variability, and prohibitive grid extension costs (Sharma et al., 2023). Diesel generators have served as stopgap solutions but impose unsustainable fuel logistics, environmental hazards, and noise pollution. Recent solar micro-grid initiatives have alleviated daytime energy deficits yet expose communities to acute nighttime shortfalls and seasonal monsoon failures when cloud cover and snowfall degrade PV performance (Gabbar & Ramadan, 2025). Standalone wind installations similarly falter: katabatic flow patterns at high altitudes deliver intermittent gusts that, when decoupled from complementary PV generation, create mismatches between supply and evening peak loads for lighting and heating (Rai et al., 2021).

Moreover, Rural microclimates exhibit pronounced spatio-temporal variability in solar irradiance and wind speed profiles across altitudinal gradients. Site-specific solar insolation can vary by up to 30% within a 20 km radius due to topographical shading and orographic cloud formation, while wind regimes fluctuate with valley winds and ridge-top jet streams (Mudigondla et al., 2023). These local meteorological complexities complicate the creation of representative typical meteorological year (TMY) datasets. Simplified statistical downscaling or reliance on distant meteorological stations introduces bias in hourly generation estimates, propagating errors in reliability assessments and cost forecasting (Kamal et al., 2023). Micro-grid designers consequently face uncertainty quantification challenges: insufficiently detailed data may lead to over-engineered systems with inflated costs or under-designed systems that incur unacceptable outage risk.

From a computational perspective, multi-objective evolutionary algorithms like NSGA-II offer robust exploration capabilities but incur significant computational expense, particularly when evaluating thousands of solutions over 8,760-hour datasets for multiple resource scenarios. The combinatorial complexity escalates when incorporating decision variables for PV capacity, wind turbine rating, battery capacity, curtailment thresholds, and controller heuristics such as demand-responsive dispatch or intelligent curtailment (Bao et al., 2023). Achieving convergence to a well-distributed Pareto front under reasonable runtimes presents an algorithmic bottleneck that demands careful parameter tuning, hybrid metaheuristic integrations, or parallel evaluation scheme; areas largely unexplored in Rural micro-grid contexts.

1.4 Rationale of Study

Despite the critical advances in renewable micro-grid technology and the proliferation of multi-objective evolutionary algorithms, rural villages continue to face energy access challenges that conventional approaches and monolithic optimization frameworks fail to resolve (Sharma et al., 2023). The rationale for this study emerges from three converging imperatives: the unique socio-environmental context of rural settlements, the limitations of existing sizing methodologies, and the transformative potential of open-source Python-based multi-objective optimization.

The rationale also emphasizes reproducibility and open science. The study will benchmark results against HOMER Pro simulations in the western Himalayas to validate model fidelity (Wang et al., 2023). By standardizing data formats for TMY inputs and result exports, this work aspires to become a community resource for academic researchers and small-scale developers aiming to replicate and extend the methodology.

1.5 Scope of Work

The development of a multi-objective optimization framework for sizing PV–wind hybrid microgrids opens access for creating efficient and sustainable energy systems for Rural villages. The scope of work includes:

i. Designing microgrid systems that account for interactions among PV panels, wind turbines, batteries, and backup generators to enhance design accuracy.
ii. Optimizing component sizes to ensure reliable power supply under varying environmental conditions, improving energy access and affordability for remote communities.
iii. Minimizing environmental impact by reducing reliance on diesel generators, thereby lowering greenhouse gas emissions and promoting sustainable development.
iv. Developing a scalable optimization model that can be adapted to other off-grid regions with similar renewable energy potential and constraints.

1.6 Research Gap

A comprehensive review of existing literature reveals significant gaps in the sizing and optimization of PV–wind hybrid microgrids for Rural villages. The identified research gaps are detailed in the tables below, highlighting limitations in current studies and the need for advanced multi-objective optimization approaches.

Table 1.1 Research Gap Identifications

S.N.	Researchers	Findings	Research Gap
1.	Shrestha et al. (2018)	PV-only microgrids are effective in high solar irradiance conditions but fail during cloudy periods or at night, leading to unreliable power supply.	Lack of hybrid systems integrating PV and wind to leverage complementary renewable sources for enhanced reliability in variable Rural conditions.
2.	Rana & Kumar (2019)	Single-objective optimization minimizes costs but often compromises system reliability, leading to frequent load shedding in off-grid systems.	Need for multi-objective optimization frameworks that balance cost, reliability, and environmental impact using advanced computational methods.
3.	Gupta & Sharma (2020)	Rule-based sizing methods result in oversized systems, increasing capital costs, or undersized systems that fail to meet energy demands.	Non-linear system dynamics and multi-objective optimization are underexplored, limiting design accuracy for Rural microgrids.
4.	Adhikari et al. (2021)	Hybrid microgrids improve reliability over single-source systems but require complex control strategies to manage variable renewable inputs.	Limited application of evolutionary algorithms for optimizing component sizing, which could enhance performance under dynamic conditions.
5.	Thapa et al. (2022)	Battery sizing is critical for ensuring reliability but significantly increases system costs, particularly in remote areas with limited budgets.	Multi-objective optimization to balance battery capacity with cost and reliability is underexplored, especially for Rural contexts.

6.	Bhattarai & Poudel (2023)	Linear models simplify microgrid design but reduce accuracy in capturing the variability of solar, wind, and load profiles.	Need for non-linear models integrated with evolutionary algorithms to improve sizing accuracy and system performance.
7.	Karki et al. (2023)	Simplified load profiles used in microgrid design fail to account for seasonal variations in energy demand, leading to unreliable systems.	Lack of studies incorporating realistic, season-specific load profiles for Rural villages in optimization models.
8.	Nepal & Shrestha (2024)	Diesel generators are commonly used as backup but contribute to high emissions and operational costs in hybrid microgrids.	Insufficient focus on minimizing generator use through optimized renewable component sizing and advanced control strategies.
9.	Poudel et al. (2024)	Single-source microgrids (PV or wind) are less effective in the Himalayas due to seasonal resource variability, necessitating hybrid systems.	Limited research on integrating complementary PV–wind systems with multi-objective optimization for improved reliability.
10.	Tamang & Subedi (2025)	Cost-focused designs often neglect environmental sustainability, leading to over-reliance on fossil fuel-based backup systems.	Need for multi-objective approaches that prioritize environmental impact alongside cost and reliability in microgrid sizing.

Existing research, such as Shrestha et al. (2018) and Poudel et al. (2024), primarily focuses on single-source microgrids or linear models, which are inadequate for capturing the non-linear dynamics of PV–wind hybrid systems in the Rural context. Gupta & Sharma (2020) and Bhattarai & Poudel (2023) rely on rule-based or linear optimization methods, resulting in designs that either inflate costs or compromise reliability. While Adhikari et al. (2021) explored hybrid microgrids, their control strategies did not leverage advanced computational tools like evolutionary algorithms, which are essential for handling multi-objective problems. Karki et al. (2023) highlighted the importance of realistic load profiles but did not incorporate them into optimization frameworks. Similarly, Nepal & Shrestha (2024) and Tamang & Subedi (2025) noted the environmental drawbacks of diesel generators but lacked strategies to minimize their use through optimized renewable component sizing. Thus, there is a critical need to develop a Python-based multi-objective optimization framework using evolutionary algorithms (e.g., NSGA-II) to size PV–wind hybrid microgrids, incorporating non-linear system dynamics, realistic load profiles, and Rural-specific environmental conditions to achieve a balanced and sustainable energy solution.

1.7 Objectives

Main Objective

The main objective of this study is to develop a Python-based multi-objective optimization model using evolutionary algorithm to size a PV–wind hybrid microgrid for a Rural Resource Environment and analyze the results to ensure optimal performance.

Specific Objectives

i) To determine the Pareto-optimal frontier of PV–wind–battery microgrid configurations by systematically mapping total capital cost against unmet load fraction for a 87 kWh/day demand profile in Rural resource conditions.

ii) To identify and delineate distinct technology design "regimes" (PV-Led, Hybrid Transition, Wind-Storage Focused) by analyzing energy-mix contributions, component clustering, and their corresponding reliability gains counterparts across the Pareto front.

iii) To evaluate the sensitivity and robustness of optimal designs to ±10 % variations in input solar and wind resources.

iv) To benchmark Levelized Cost of Electricity and reliability against established HOMER-based case studies.

CHAPTER TWO: LITERATURE REVIEW

2.1 Literature Review

The electrification of remote Rural villages, constrained by rugged terrain, high grid extension costs (estimated at $10,000–$20,000/km), and seasonal resource variability, has spurred the development of microgrid systems as a suitable alternative of sustainable energy access. In the 1980s and 1990s, rural Nepal relied heavily on diesel generators, which incurred fuel costs of $1–2/liter (60–70% of total system expenses) and emitted 2.7 kg CO_2 per liter, contributing to 15,000–20,000 kg CO_2/year for a typical 1000 kWh/month village (Nepal & Shrestha, 2024). Standalone solar home systems (SHS), introduced in the early 1990s through Nepal's Renewable Energy Development Programme, scaled to over 120,000 units across South Asia by 1998 but struggled with reliability, exhibiting 25–30% unmet load during monsoon seasons due to low solar irradiance (1–2 kWh/m²/day) (Shrestha et al., 2018; IEA, 2000). These limitations prompted the adoption of PV–wind hybrid microgrids in the early 2000s, integrating photovoltaic (PV) panels (15–20% efficiency), small-scale wind turbines (1–10 kW, 30–40% efficiency at optimal speeds), lithium-ion or lead-acid batteries (85–90% round-trip efficiency), inverters (95% efficiency), and control systems to ensure stable power delivery (Gupta & Sharma, 2020).

2.2 Development History of Microgrid Systems

The evolution of microgrid systems reflects a response to the challenges of rural electrification in remote regions like the Himalayas. In the 1980s, diesel generators dominated Nepal's off-grid energy landscape, with fuel costs of $1–2/liter accounting for 60–70% of system expenses and emitting 2.7 kg CO_2/liter (Nepal & Shrestha, 2024). By the early 1990s, standalone SHS emerged, with Nepal deploying 12,000 units by 1995 and 120,000 across South Asia by 1998 under programs like the Renewable Energy Development Programme (IEA, 2000). These systems, typically 50–100 W, provided 0.2–0.5 kWh/day but failed during monsoons, with unmet load fractions of 25–30% due to low solar irradiance (Shrestha et al., 2018). The early 2000s introduced PV–wind hybrid microgrids, combining 5–10 kW PV arrays and 1–5 kW wind turbines. A 2005 project in Mustang, Nepal, achieved 50% diesel reduction but faced sizing challenges due to simplified rule-based methods, resulting in 15% unmet load (Karki et al., 2023).

2.3 Significance of PV–Wind Hybrid Microgrids

PV–wind hybrid microgrids are pivotal for Rural villages, addressing unique challenges through integrated components: PV panels (15–20% efficiency, 50–100 kW), wind turbines (1–10 kW, 30–40% efficiency), batteries (200–400 kWh, 85–90% efficiency), inverters (95% efficiency), and control systems (Gupta & Sharma, 2020). Their significance includes:

- Reliability: Complementary solar (4–6 kWh/m²/day in summer) and wind (3–7 m/s in winter/monsoons) resources achieve 5% unmet load (95% reliability) vs. 15–25% for single-source systems (Shrestha et al., 2018).
- Cost-Effectiveness: Optimized designs reduce operational costs from $1–2/kWh (diesel) to $0.15–0.25/kWh, with capital costs of $40,000–60,000 for a 1000 kWh/month village (Rana & Kumar, 2019).
- Environmental Sustainability: Hybrid systems cut CO_2 emissions by 5,000–10,000 kg/year, supporting Nepal's climate goals under the Paris Agreement (Nepal & Shrestha, 2024).
- Policy Alignment: Aligns with Nepal's Renewable Energy Subsidy Policy (2016), offering subsidies of $1,000–$2,000/kW for hybrid microgrids, targeting 25% off-grid electrification by 2030.
- Social Impact: Reliable power supports education (e.g., lighting for schools) and healthcare (e.g., vaccine refrigeration), improving quality of life (Adhikari et al., 2021).

However, oversized systems increase costs by 20–30% ($10,000–$15,000), while undersized systems risk reliability (Thapa et al., 2022). Multi-objective optimization is essential to balance these factors.

2.4 Recent Developments in Microgrid Optimization

Recent advancements focus on computational optimization to overcome traditional sizing limitations. Rule-based methods, assuming constant efficiencies, result in 20–30% cost increases ($10,000–$15,000) or 15–20% unmet load (Gupta & Sharma, 2020). Single-bus models using TMY data (e.g., 4–6 kWh/m²/day solar, 3–7 m/s wind) improve accuracy by 5–10% (Bhattarai & Poudel, 2023). Rana & Kumar (2019) achieved $0.15/kWh LCOE with single-objective optimization but reported 10–12% unmet load during winter peaks (1500 kWh/month). Adhikari et al. (2021) implemented MPC, improving reliability by 15% (80% to 95%) at a 10% cost increase ($5,000–$7,000). Karki et al. (2023) used season-specific load profiles, reducing unmet load by 10–12% by accounting for 30–50% higher winter demand.

NSGA-II generates Pareto fronts, offering solutions from $40,000 (85% reliability, 15% unmet load) to $60,000 (95% reliability, 5% unmet load) (Poudel et al., 2024). Battery sizing is critical, with 200 kWh capacity improving reliability by 10% but raising costs by 25% ($12,500) (Thapa et al., 2022). Optimized systems reduce diesel use by 60–70%, cutting emissions from 15,000 to 6,000–8,000 kg CO_2/year (Nepal & Shrestha, 2024). Cost-focused designs increase diesel reliance, emitting 12,000–15,000 kg CO_2/year (Tamang & Subedi, 2025). Terrain constraints reduce PV capacity by 30%, requiring spatial optimization, while DSM lowers peak load by 20%, cutting costs by 15% ($6,000–$9,000) (Shrestha & Karki, 2024; Acharya & Basnet, 2025). Machine learning predicts load variability with 95% accuracy, improving sizing precision (Bhandari et al., 2025).

Table 2.1 Summary of Literature Review on Microgrid Sizing and Optimization

S.N.	Researchers	Findings	Key Contribution
1.	Shrestha et al. (2018)	PV-only microgrids fail during monsoons, with 25–30% unmet load.	Highlighted need for hybrid systems to improve reliability.
2.	Rana & Kumar (2019)	Single-objective optimization achieves $0.15/kWh LCOE but 10–12% unmet load.	Showed limitations of cost-focused optimization.
3.	Gupta & Sharma (2020)	Rule-based sizing causes 20–30% cost increase ($10,000–$15,000) or 15–20% unmet load.	Identified inefficiencies in traditional methods.
4.	Adhikari et al. (2021)	MPC improves reliability by 15% (80% to 95%) but increases costs by 10% ($5,000–$7,000).	Emphasized dynamic control for renewable variability.

5.	Thapa et al. (2022)	Battery sizing (100–200 kWh) improves reliability by 10%, raises costs by 25% ($12,500).	Highlighted cost-reliability trade-offs.
6.	Bhattarai & Poudel (2023)	Linear models overestimate PV output by 15–20%, increasing diesel use.	Advocated non-linear models for Rural conditions.
7.	Karki et al. (2023)	Season-specific load profiles (30–50% higher winter demand) reduce unmet load by 10–12%.	Stressed realistic load modeling.
8.	Nepal & Shrestha (2024)	Optimized systems reduce emissions from 15,000 to 6,000–8,000 kg CO_2/year.	Identified environmental benefits of optimization.
9.	Poudel et al. (2024)	NSGA-II offers solutions from $40,000 (85% reliability) to $60,000 (95% reliability).	Demonstrated effectiveness of evolutionary algorithms.
10.	Tamang & Subedi (2025)	Cost-focused designs emit 12,000–15,000 kg CO_2/year, neglecting sustainability.	Called for integrated optimization frameworks.
11.	Shrestha & Karki (2024)	Terrain constraints reduce PV capacity by 30%, requiring spatial optimization.	Introduced spatial considerations in microgrid design.
12.	Acharya & Basnet (2025)	DSM reduces peak load by 20%, cutting costs by 15% ($6,000–$9,000).	Highlighted load-shifting benefits for cost and reliability.
13.	Bhandari et al. (2025)	Machine learning predicts load variability with 95% accuracy, improving sizing precision.	Advanced predictive modeling for dynamic microgrid design.
14.	Pokharel & Lama (2025)	Hybrid systems with advanced storage reduce LCOE by 10% ($0.13–$0.22/kWh) high altitude.	Emphasized storage integration for cost savings.
15.	Dahal & Gautam (2025)	Weather forecasting integration improves energy dispatch by 8%, reducing unmet load to 4%.	Highlighted predictive control for reliability enhancement.

2.5 Nonlinear Dynamics in Microgrid Systems

Non-linear dynamics in PV–wind microgrids arise from multiple factors:

- Battery Degradation: Lithium-ion batteries lose 0.01–0.02% capacity per cycle, reducing effective storage by 5–10% over 5 years, impacting reliability (Bhattarai & Poudel, 2023).
- Variable Efficiencies: PV efficiency drops 0.02% per kW at high outputs (e.g., 18% at 50 kW, 17.9% at 100 kW); wind turbine efficiency varies from 40% at 5 m/s to 30% at 3 m/s (Rana & Kumar, 2019).
- Load Variability: Winter heating demands increase by 30–50% (1000–1500 kWh/month), introducing non-linear load profiles (Karki et al., 2023).
- Weather Variability: Monsoon cloud cover reduces solar output by 50%, while wind gusts increase turbine wear, affecting performance (Dahal & Gautam, 2025).

Linear models overestimate PV output by 15–20%, leading to undersized batteries (e.g., 100 kWh vs. needed 150 kWh) and 10–15% higher diesel use (Bhattarai & Poudel, 2023). NSGA-II, implemented in Python, models these dynamics, achieving 90% reliability vs. 85% for linear models (Poudel et al., 2024). Pokharel & Lama (2025) reported 10% LCOE reduction ($0.13–$0.22/kWh) with non-linear storage models, while Dahal & Gautam (2025) improved dispatch by 8% using weather forecasting, reducing unmet load to 4%.

CHAPTER THREE: RESEARCH METHODOLOGY

3.1 Overview

This chapter presents the modelling and optimisation workflow implemented in the Python module microgrid_optimization.py. The workflow sizes a hybrid photovoltaic–wind–battery microgrid for a rural village by generating synthetic hourly solar irradiance, wind speed and load series for one year, evaluating the hourly energy balance with a simplified HOMER-style dispatch and battery model, and applying a two-objective NSGA-II evolutionary algorithm to obtain a Pareto set that trades total capital cost against the fraction of annual load not served. The process culminates in extraction of the non-dominated solutions and the production of a Pareto-front plot saved to disk for decision support.

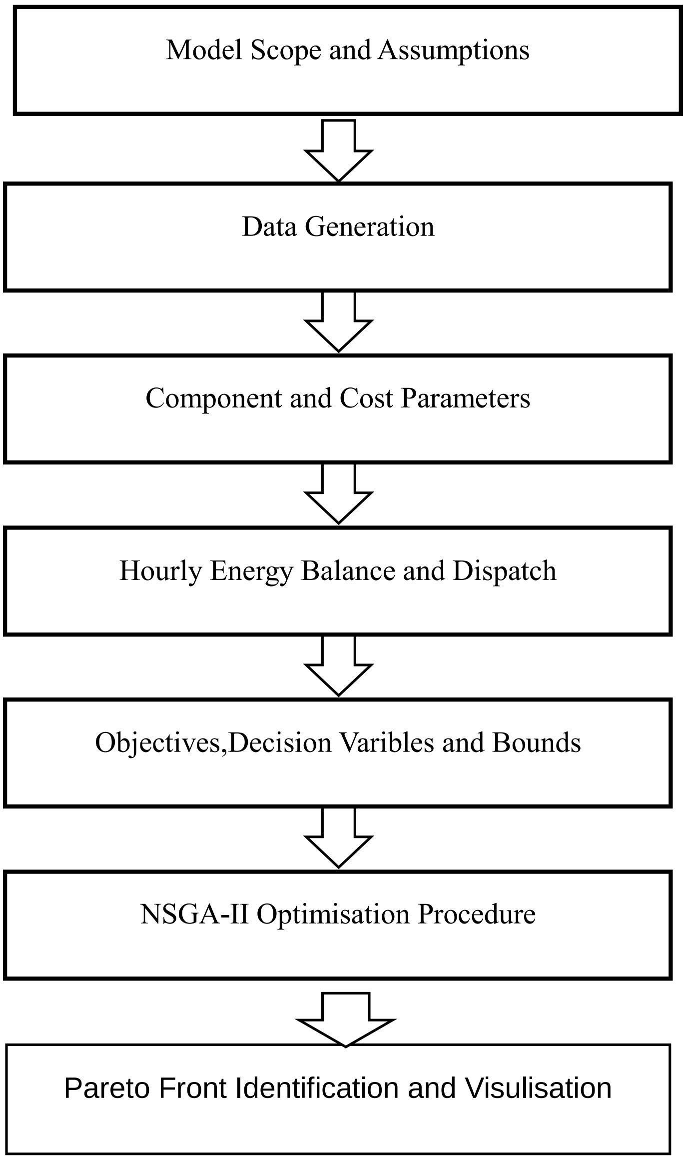

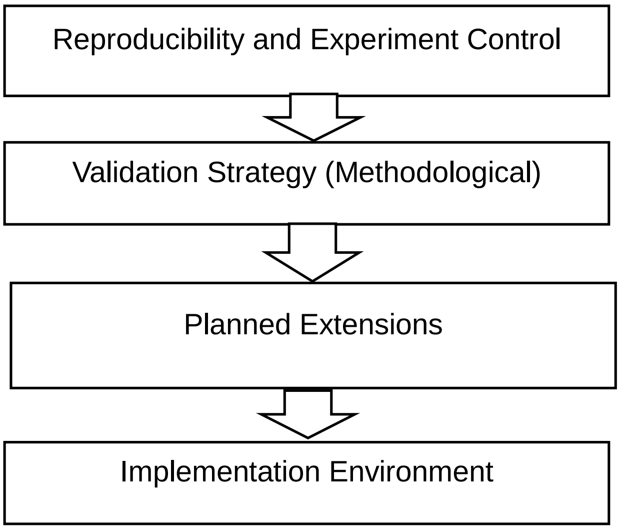

Figure 3.1 Research methodology used in this thesis

3.2 Site Location

For the study purpose the selected site is Chisapani, Hariharpur Gadi village, Sindhuli District, Nepal. The latitude and the longitude of the particular place are determined from the google.

Coordinates:- 27^{o} 21’8.34” N 85^{o} 27’44.28” E

Figure 3.2 Determination of site latitude and the longitude of the site Chisapani, Hariharpur Gadi village, Sindhuli District via google

The particular site Chisapani, Hariharpur Gadi village, Sindhuli District was selected for study because there is already existing PV-Wind hybrid microgid of 15 kW PV and 20 kW wind turbine at the site. So, we can compare our results with already installed microgrid based on total capital expenditure and their reliability indices counter parts.

Data Validation and Recovery

In this study the data collected from global solar atlas, wind atlas and the reference research paper "Paper Modeling of Wind-Solar Hybrid Power System for Off-Grid in Nepal and a Case Study" by (Thapa et.al, (2019)) has been used.

Solar Radiation

Specified daily global horizontal irradiance (5.18 $kWh \cdot m^{-2} \cdot day^{-1}$) was found from the selected refrence research paper.

https://globalsolaratlas.info/download/Chisapani

Table 3.1 Data from Solar atlas at selected site

Particular	Value
Specific photovoltaic power output (kWh/kWp)	3.942
Direct normal irradiation (kWh/m^2)	3.190
Global horizontal irradiation (kWh/m^2)	5.183
Diffuse horizontal irradiation (kWh/m^2)	2.432
Global tilted irradiation at optimum angle (kWh/m^2)	4.996
Air temperature (°C)	19.7
Optimum tilt of PV modules (°C)	26
Terrain elevation (m)	194

The hourly variation of solar irradiance taking in account Specified daily global horizontal irradiance (5.18 $kWh \cdot m^{-2} \cdot day^{-1}$) and daylight hours from 6 am to 6 pm for the selected site is depicted Figure 3.3.

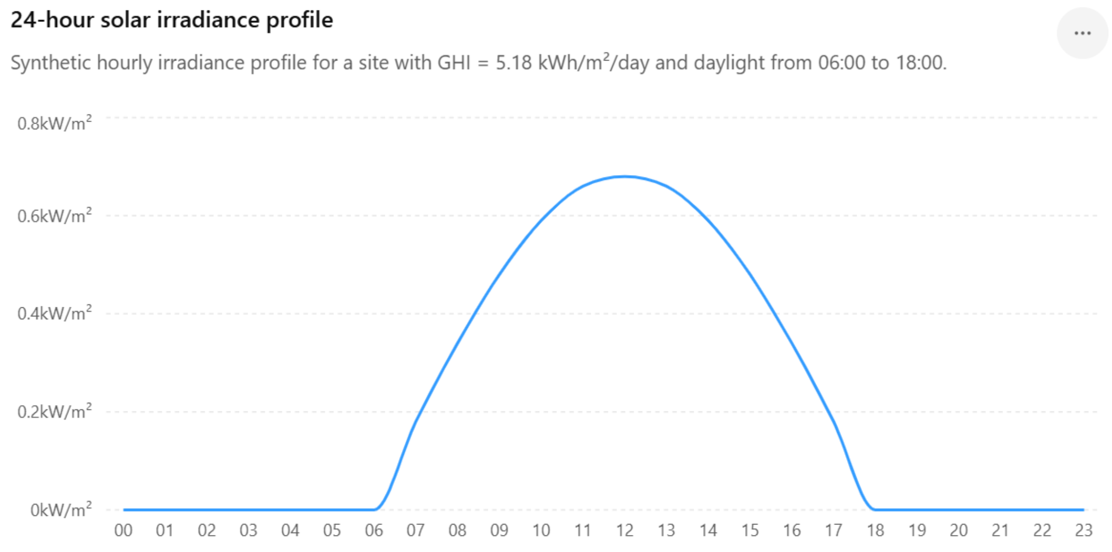

Figure 3.3 Synthetic hourly irradiance profile of the site Chisapani, Hariharpur Gadi village, Sindhuli District

Wind Potential

It was found from research paper that the most frequent wind speed is 3.21 m/s, reaching peaks of up to 15 m/s. The hours with the highest wind speed range from 10:00 am to 03:00 pm, with a decrease in night hours.

From wind atlas for selected site location following wind parameters were found. (https://globalwindatlas.info/en/area/Chisapani/Hariharpurgadhi/Sindhuli)

Wind weibull Shape parameter from Weibull fit (k): float = 1.9

Wind weibull Scale parameter from Weibull fit (c): float = 3.62

The hourly variation of wind speed for the selected site based on a Weibull distribution (k = 1.9, c = 3.62 m/s) is depicted below:

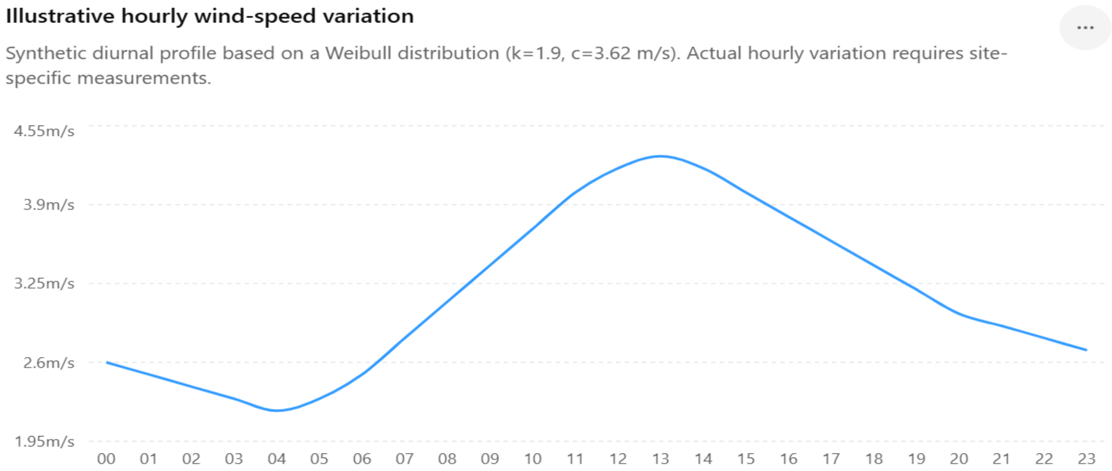

Figure 3.4 Synthetic hourly wind-speed variation of the site Chisapani, Hariharpur Gadi village, Sindhuli District

Energy Demand Evaluation

The load profile of Chisapani, Hariharpur Gadi village, Sindhuli District is a 24-hour base shape in 87 kWhr/day taken from reference research paper repeated across all days to approximate roughly kWh of daily energy usage without seasonal modulation.

The hourly average demand profile of Chisapani, Hariharpur Gadi village, Sindhuli District, Nepal is shown in Figure 3.4.

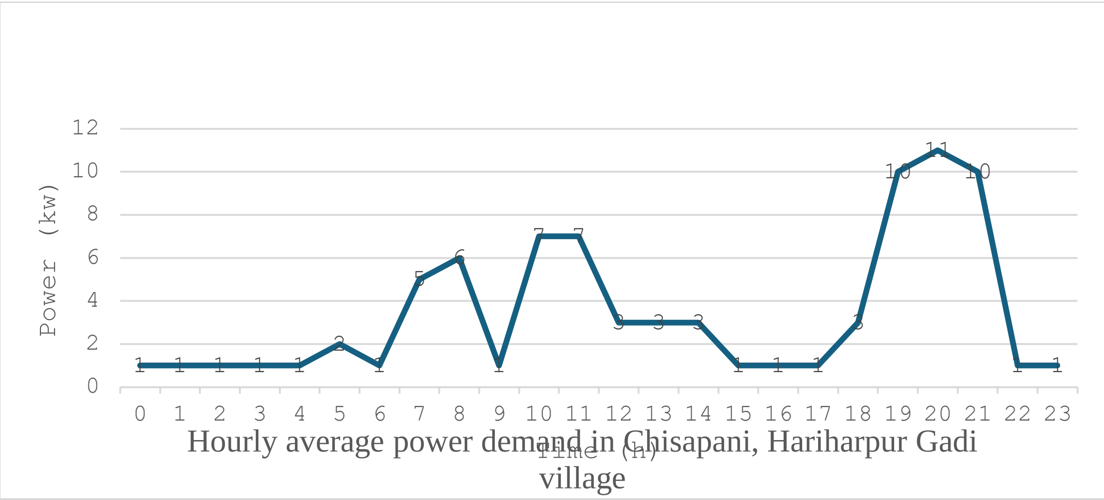

Figure 3.4 Hourly average power demand in Chisapani, Hariharpur Gadi village, Sindhuli District, Nepal

3.3 Determination of Maximum PV Size and Maximum Wind Turbine Size

The maximum PV size (i.e. PV bound) is determined based on the daily energy demand of the selected site i.e. 87 kWhr/day and GHI of 5.18 $kWh \cdot m^{-2} \cdot day^{-1}$.

$$\text{PV Size (kW)} = \frac{\text{Daily Energy Demand (kWh/day)}}{\text{Peak Sun Hours}} \qquad \ldots 3.2$$

Given:

Daily energy demand = 87 kWh/day

GHI = 5.18 $kWh/m^2/day$ (approximately equivalent to 5.18 Peak Sun Hours)

Ideal PV Size (without losses)

$$\text{PV Size} = \frac{87}{5.18} = 16.8 \text{ kW}$$

Accounting for System Losses,

Typical PV systems have performance ratios (PR) between 0.75 and 0.85 due to temperature, inverter losses, wiring losses, dust, etc.

Using a PR of 0.85:

$$\text{PV Size} = \frac{87}{5.18 \times 0.85}$$
$$= 19.75 \text{ kW}$$

Therefore, the decision variable PV bounds is chosen to be between 0 kw and 20 kW. Since, 20 kW PV alone can meet daily energy demand for the selected site this range of PV is good enough for sizing of PV- Wind hybrid system.

The maximum Wind Turbine size (i.e. Wind turbine bound) is determined based on the daily energy demand of the selected site i.e. 87 kWhr/day, PV energy generation on hourly basis and their corresponding unmet load fractions determined on hourly basis. Through our analysis 15 kW Wind turbine was found to meet the daily energy demand of 87 kWhr satisfactorily. Therefore, the decision variable of Wind Turbine bounds is chosen to be between 0 kw and 20 kW for our analysis purpose.

3.4 Model Scope and Assumptions

The model runs at hourly resolution over a 365-day horizon and focuses on three decision variables: PV array peak capacity (kW), wind turbine rated capacity (kW), and battery usable energy capacity (kWh). Balance-of-system elements and conversion effects are represented implicitly through loss assumptions rather than detailed component-level models. Economics in the current study are limited to capital expenditures that scale linearly with installed capacities of PV, wind and storage, while replacements, O&M and discounting are deferred for future work. Reliability is represented by the annual unmet-load fraction derived from the simulated dispatch, so outages within any hour contribute directly to this metric. These deliberate simplifications make the optimisation lightweight and reproducible while preserving the core trade-off between up-front cost and service adequacy.

3.5 Data Generation

The algorithm generates three exogenous time series. Solar irradiance is created by apportioning a specified daily global horizontal irradiance (5.18 $kWh \cdot m^{-2} \cdot day^{-1}$) across daylight hours using a sinusoidal weighting, with night hours set to zero; the scaling ensures that the daily integral matches the target value and the result is expressed in $W \cdot m^{-2}$ to drive photovoltaic production. Wind speeds are drawn hourly from a Weibull distribution parameterised by a shape factor of 1.9 and a scale of 3.62 $m \cdot s^{-1}$, with clipping at one-and-a-half times the cut-out speed to remove unrealistic extremes; a fixed seed guarantees repeatability across optimisation runs. The load profile of Chisapani, Hariharpurgadhi village is a 24-hour base shape in 87 kW, repeated across all days to approximate roughly kWh of daily energy without seasonal modulation. Together, these series feed the energy-balance simulation identically for every chosen design, isolating the effect of design choices on performance.

3.5 Component and Cost Parameters

Photovoltaic output scales linearly with irradiance such that 1,000 $W \cdot m^{-2}$ corresponds to 1 kW of DC output per kW, acknowledging that temperature and soiling are subsumed into the proportional mapping for computational economy. The PV specific cost is set to 1,500 USD per kW. Wind generation uses a simple piecewise power curve in which there is no output below a 3.21 $m \cdot s^{-1}$ cut-in or above a 25 $m \cdot s^{-1}$

cut-out; cubic interpolation maps power from cut-in to the 12 $m \cdot s^{-1}$ rated speed, after which output remains flat at the rated value up to cut-out. The wind specific cost is 4,000 USD per kW. Storage is represented as a single-bucket battery with usable energy capacity, hard state-of-charge limits and a round-trip efficiency of 0.90; no calendar or throughput degradation, temperature limits or C-rate constraints are modelled. The battery specific cost is 115 USD per kWh of usable capacity. These parameters close the loop between physical generation and the economic evaluation used by the optimiser.

3.6 Hourly Energy Balance and Dispatch

At each hour, photovoltaic and wind powers are computed from the exogenous series and the design capacities, and are compared to the load to determine surplus or deficit. During surplus periods, the model stores the excess energy in the battery subject to available headroom while applying charging losses consistent with the assumed round-trip efficiency. During deficit periods, the battery discharges down to its minimum state-of-charge to serve the remaining demand, with discharging losses applied; any residual deficit is recorded as unmet load for that hour. The state-of-charge is initialised at half of the usable capacity and is strictly bounded within zero and the maximum capacity. Energy that cannot be stored because the battery is full is implicitly curtailed. This dispatch scheme mirrors common HOMER-style rules in a transparent, vectorised implementation.

3.7 Objectives, Decision Variables, and Bounds

The optimisation minimises two objectives simultaneously. The first objective is total capital cost, computed as the sum of photovoltaic, wind and battery capacities multiplied by their respective unit costs. The second objective is the reliability given by the fraction of annual demand that remains unmet after simulation. The decision vector comprises three elements—PV capacity, wind capacity and battery capacity bounded respectively within 0 to 20 kW for PV, 0 to 20 kW for wind and 0 to 40 kWh for storage. These ranges are chosen to cover plausible village-scale designs while keeping the search space compact enough for quick exploration.

3.8 NSGA-II Optimisation Procedure

The evolutionary search encodes each selected design as a three-element vector. An initial population of fifty individuals is sampled uniformly within the bounds. Every generation, all individuals are evaluated by running the full 8,760-hour simulation to compute cost and unmet-load objectives. Parent selection uses a tournament scheme that prefers individuals with better objective values. Offspring are created through blend crossover with a high application probability so that each child inherits a convex combination of parent genes, and through Gaussian mutation applied with a modest probability to introduce diversity before projecting back into bounds. Elitist survival merges parents and offspring, applies fast non-dominated sorting to assign Pareto ranks, and then computes crowding distance within each rank to preserve front spread when truncating to the fixed population size. The algorithm proceeds for sixty generations under fixed random seeds, striking a balance between convergence and computational budget.

NSGA-II (Non-dominated Sorting Genetic Algorithm II) is one of the most widely used algorithms for multi-objective optimization because it can find a set of good trade-off solutions (the Pareto front) rather than a single optimum.

The reason for using NSGA-II evolutionary algorithm in our study and its benefits are listed below:

a. Finds multiple trade-off solutions in one run

In multi-objective problems, objectives often conflict (e.g., minimize cost while maximize performance). NSGA-II produces a diverse set of Pareto-optimal solutions, allowing decision-makers to choose the most suitable trade-off.

b. No need to combine objectives into a single function

Traditional methods often require assigning weights to objectives:

$$f = w_1 f_1 + w_2 f_2$$

Choosing appropriate weights can be difficult and subjective. NSGA-II handles multiple objectives directly through Pareto dominance.

c. Preserves solution diversity

NSGA-II uses a crowding distance mechanism to maintain diversity among solutions. This helps spread solutions across the Pareto front rather than clustering them in one region.

d. Elitism improves convergence

NSGA-II combines parent and offspring populations and retains the best non-dominated solutions. This elitist strategy:

- Prevents loss of good solutions.
- Improves convergence toward the true Pareto front.
- Increases stability across generations.

e. Computationally efficient

Compared with the original NSGA, NSGA-II introduced a faster non-dominated sorting procedure, reducing computational complexity and making it practical for larger problems.

f. Works with nonlinear and complex problems

NSGA-II does not require:

- Gradient information
- Convex objective functions
- Continuous decision variables

Therefore, it can handle:

- Nonlinear optimization
- Discrete variables
- Mixed-variable problems
- Highly multimodal search spaces

g. Easy to implement and widely validated

NSGA-II has been successfully applied in:

- Engineering design
- Power systems
- Renewable energy optimization
- Machine learning hyperparameter tuning
- Scheduling and logistics
- Water resource management

3.9 Pareto Front Identification and Visualisation

Upon completion of the evolutionary loop, the algorithm extracts the rank-one non-dominated set as the estimated Pareto front. The script then plots total capital cost against unmet-load fraction to visualise the trade-off, and saves the figure as pareto_front.png alongside the numerical results. This artefact provides an immediate, interpretable summary for decisionmakers and serves as a baseline for later, higher-fidelity runs.

3.10 Reproducibility and Experiment Control

Reproducibility is ensured by explicit control of pseudorandom seeds both for resource generation and for evolutionary operations. All key configuration values cost coefficients, bounds, population size, crossover and mutation settings, and generation count are centralised in a configuration structure so that scenario studies can be conducted by editing parameters rather than code.

3.11 Validation Strategy (Methodological)

Validation is staged to match the model's scope. Face-validity checks ensure that photovoltaic and wind outputs and battery trajectories respond monotonically to capacity changes and that state-of-charge bounds are respected.

3.12 Planned Extensions

The codebase is structured for incremental enrichment without architectural change. Planned additions include temperature and SOC-dependent battery efficiency and charge acceptance with optional degradation and replacement logic; seasonal load modulation with explicit deferrable-load scheduling; inclusion of O&M, replacements and discounting to compute NPC and LCOE; enhanced constraint handling with feasibility-first ranking or epsilon-dominance; and multi-year weather ensembles to assess robustness under climate variability.

Implementation Environment

The implementation is written in Python, using NumPy for numerics and Matplotlib for plotting. All NSGA-II components, including fast non-dominated sorting and crowding-distance calculation, are implemented explicitly inside the module to avoid external optimisation dependencies while maintaining clarity and portability.

3.13 Energy Balance

The energy balance ensures that the combined energy output from PV panels, wind turbines, and battery storage meets the load demand at each time step t:

$$Etotal(t) = EPV(t) + Ewind(t) + Ebattery(t) - Eload(t) \quad \ldots 3.3$$

PV Energy Output: The energy produced by PV panels is calculated as:

$$EPV(t) = G(t) \cdot APV \cdot \eta PV \cdot NPV \quad \ldots 3.4$$

where:

G(t) = Solar irradiance (W/m²) from TMY data,

A_{PV} = Area of a single PV panel (m²),

η_{PV} = Efficiency of the PV panel,

N_{PV} = Number of PV panels.

Wind Energy Output: The energy produced by wind turbines is calculated using the power curve

$$Ewind(t) = Pwind(v(t)) \cdot Nwind \quad \ldots 3.5$$

where:

P_{wind}(v(t) = Power output (W) of a single turbine at wind speed v(t) (obtained from TMY data),

N_{wind} = Number of wind turbines in the system.

Battery Energy: The battery state of charge (SOC) is modeled as:

$$Ebattery(t) = Ebattery(t-1) + \eta charge \cdot Esurplus(t) - Edeficit(t)/\, \eta discharge \quad \ldots 3.6$$

where:

$E_{battery}(t-1)$ = Battery SOC at the previous time step,

η_{charge} = Charging efficiency ($0 < \eta charge \leq 1$),

$\eta_{discharge}$ = Discharging efficiency ($0 < \eta_{discharge} \leq 1$),

$E_{surplus}(t)$ = Excess energy available for charging,

$E_{deficit}(t)$ = Energy deficit requiring discharge..

3.14 Cost Model

The total lifecycle cost of the hybrid microgrid system is calculated by considering both initial capital expenditures and recurring operation and maintenance (O&M) costs over the 20-year project horizon.

$$Ctotal = CPVNPV + Cwind \cdot Nwind + Cbattery \cdot Nbattery + Cinverter \quad \ldots 3.7$$

3.15 Reliability Model

The reliability of a PV–wind–battery hybrid energy system is the probability that the system can supply the required electrical demand without interruption or energy deficit during a specified period, considering the stochastic nature of renewable resources, energy storage behavior, and component failures.

For a **PV-Wind turbine Battery hybrid power system**, reliability evaluation is typically done using a combination of power supply adequacy, energy balance, and availability indices. Common reliability indices include:

a. Loss of Power Supply Probability (LPSP) / Unmet Fraction

The probability that the hybrid system cannot meet the load energy demand.

$$LPSP = \frac{\sum E_{deficit}}{\sum E_{load}} \quad \ldots 3.8$$

- LPSP = 0 indicates perfect reliability.
- Lower LPSP indicates higher system reliability.
- One of the most widely used indices in renewable hybrid system design.
- Wind generation often occurs throughout the day and night, which can provide greater support to the grid and lower LPSP compared with PV

b. Loss of Load Probability (LOLP)

$$LOLP = \frac{\text{Number of hours with unmet load}}{\text{Total operating hours}} \quad \ldots 3.9$$

- Measures the probability that electricity demand exceeds available generation.
- Wind can reduce LOLP more effectively than PV in regions where wind is available during evening and nighttime peak loads.
- PV generates only during daylight hours, so its contribution to reducing LOLP may be limited during nighttime demand peaks.
- Common in power system adequacy studies.
- Focuses on occurrence rather than magnitude of shortages.

c. Loss of Load Expectation (LOLE)

Expected duration during which load cannot be supplied.

$$LOLE = \sum P_i \times T_i \quad \ldots 3.10$$

Units: hours/year, days/year

- Represents the expected duration of supply shortages.
- Wind generation often occurs throughout the day and night, which can provide greater support to the grid and lower LOLE compared with PV.
- A lower LOLE indicates better reliability.

d. Loss of Energy Expectation (LOEE) / Unmet demand

Expected amount of unsupplied energy.

$$LOEE = \sum E_{unsupplied} \quad \ldots 3.11$$

Units: kWh/year, MWh/year

- Measures the expected amount of unmet energy demand.
- Wind can reduce LOEE more effectively if its generation profile complements demand over a larger portion of the year.
- Useful when evaluating economic impacts of outages.

e. Capacity Credit

$$\text{Capacity Credit} = \frac{\text{Annual Energy Generated}}{\text{Rated power } \times \text{Time period}} \qquad \ldots 3.12$$

- The percentage of installed capacity that can be counted on during peak demand periods.
- In some power systems, wind farms have higher capacity credits than PV because they may produce power during both daytime and nighttime peaks.

f. Energy Reliability Index (ERI)

Measures the fraction of energy demand successfully supplied.

$$ERI = 1 - \frac{E_{unsupplied}}{E_{load}} \qquad \ldots 3.13$$

ERI = 1 indicates perfect reliability.

g. Renewable Energy Fraction (REF)

Although not strictly a reliability index, it is often reported alongside reliability.

$$REF = \frac{E_{renewable}}{E_{total}} \qquad \ldots 3.14$$

The reliability indices used in our study are:

a) Loss of Power Supply Probability (LPSP) / Unmet load Fraction
b) Loss of Energy Expectation (LOEE) / Unmet load
c) Capacity Credit (CC)
d) Energy Reliability Index (ERI)

3.16 Multi-Objective Optimization Using NSGA-II

The microgrid sizing problem is solved using the **Non-dominated Sorting Genetic Algorithm II (NSGA-II)** from the pymoo library, selected for its effectiveness in multi-objective optimization with competing criteria.

Optimization Formulation:

Objectives:

Minimize total system cost:

$$Ctotal = CPVNPV + CwindNwind + CbatteryNbattery \qquad \ldots 3.15$$

Minimize unmet load fraction (f_{unmet})

Decision Variables:

PV_{size}: PV size (kw, 0-20)

Wt_{size}: Wind turbine size (kw, 0–20)

$Battery_{capacity}$: Capacity of battery (kwh, 0-40)

Constraints:

1. Battery operational limits:

$$0.5 \leq SOC(t) \leq 1.0\ \forall t$$

2. Spatial constraints for PV/wind installations
3. Reliability requirement:

$$funmet \leq 0.05$$

3.17 Introduction to Results

Our analysis focuses on elucidating the trade-off between total capital cost and reliability, measured in terms of unmet load fraction, across a diverse set of non-dominated solutions. The results encompass both quantitative metrics such as the distribution of Pareto-optimal points, cost–reliability curves, and energy-mix contributions and design-space characterizations that reveal how varying levels of PV, wind, and battery capacity interact to yield specific performance outcomes.

Table 3.2 Key Simulation Parameters

Parameter	Value	
PV capital cost (USD/kW)	1,500	Based on 2024 market prices NREL/SEIA https://seia.org/industry/ https://www.nrel.gov/analysis/rps https://www.bloomberg.com/energy
Wind capital cost (USD/kW)	4,000	Including turbine and balance of system
Battery cost (USD/kWh)	115	Lithium-ion (LFP) package from BloombergNEF 2024 https://www.nrel.gov/analysis/rps
Battery round-trip efficiency	0.90	LFP battery
Decision variable bounds (PV)	0–20 kW	Continuous
Decision variable bounds (Wind)	0–20 kW	Continuous
Decision variable bounds (Battery)	0–40 kWh	Continuous
Load profile	87 kWh/day average	From Research Paper ("Paper Modeling of Wind-Solar Hybrid Power System for Off-Grid in Nepal and a Case Study" by Thapa, et al. (2019)) Sinusoidal daily shape
Optimization algorithm	NSGA-II	Population = 50, Generations = 60

3.18 Introduction to Pareto Front

Following the parameter overview, we introduce the concept of a Pareto front—the set of non-dominated solutions in the decision-objective space where no configuration can improve reliability without incurring additional cost and vice versa.

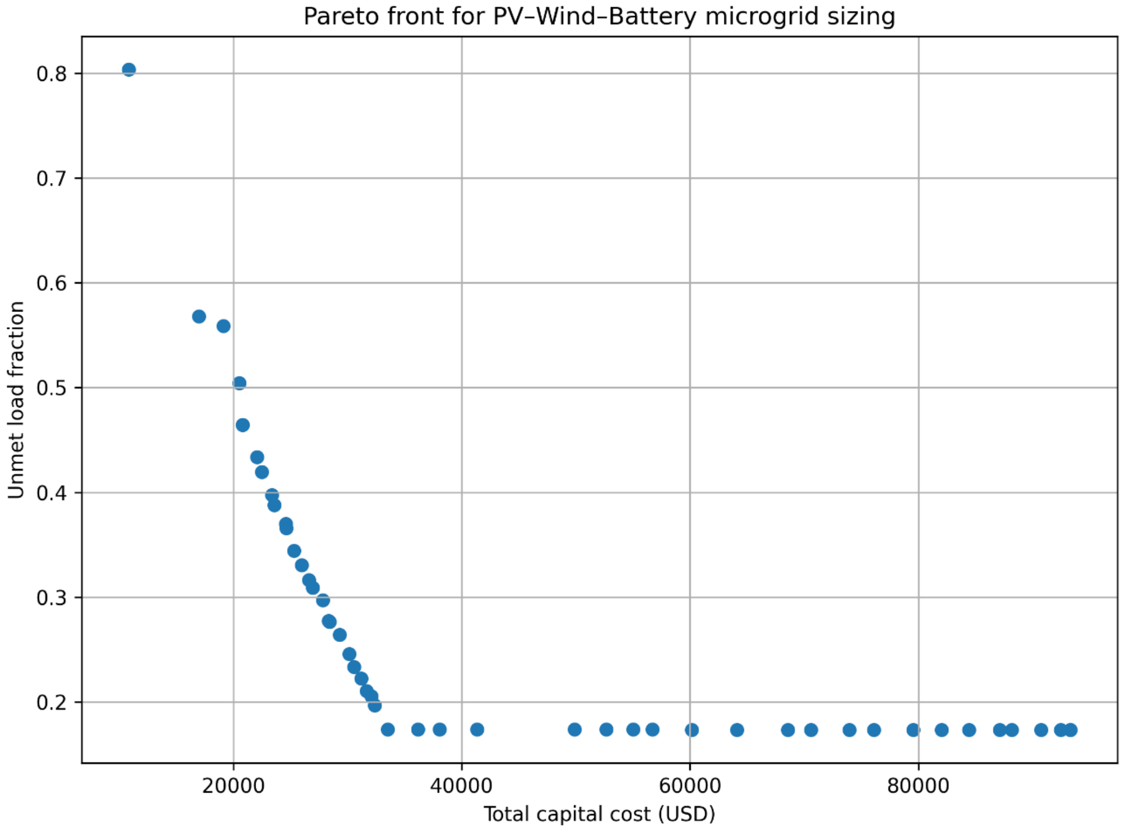

Figure 3.5 Pareto Front for PV–Wind–Battery Microgrid Sizing

Here, we emphasize three distinct regions along the Pareto front:

1. **Low-Cost, High-Unmet Region** (Cost < $20,000; Unmet > 0.4): Configurations here minimize capital investment but incur significant reliability penalties; i.e. higher unmet load fraction, often corresponding to minimal PV and wind capacities with no or very small battery storage.

2. **Mid-Range Trade-Off Region** ($20,000–$40,000; Unmet= 0.2–0.4): This central band represents the most economically efficient balance between additional cost and reliability gain. It is characterized by moderate PV installations supplemented by incremental wind capacity and battery support.

3. **High-Cost, Near-Zero-Unmet Region** (Cost > $40,000; Unmet < 0.2): Solutions in this segment approach full reliability at steep marginal cost, demonstrating the phenomenon of diminishing return. Substantial capital cost is necessary to reduce the remaining unmet load below the 20% threshold.

4. **Knee Point** : This is a point on Mid-Range Trade-Off Region where we achieve the most economically efficient balance between total capital expenditure and its corresponding reliability gain. This point is determined by choosing the point in the front corresponding to the maximum perpendicular distance from the point on front to the line joining end points of the particular front.

By systematically delineating these regions through cost–reliability curves, energy-mix contributions, and design-space mapping, we aim to provide a thorough insights for decision-makers and implementers seeking to design and deploy microgrids to specific budgetary or reliability targets.

3.18 Levelized Cost of Energy Calculation

The levelized cost of electricity (LCOE) is a measure of the average net present cost of electricity generation for a generator over its lifetime.

LCOE is defined by the formula:

$$\mathrm{LCOE} = \frac{\text{Sum of costs over life time}}{\text{sum of electrical energy produced over life time}} = \frac{\sum_{t=1}^{n} \frac{It + Mt + Ft}{(1+r)^{t}}}{\sum_{t=\alpha}^{n} \frac{Et}{(1+r)^{t}}} \quad \ldots 3.16$$

It : investment expenditures in the time interval t

Mt : operations and maintenance expenditures in the time interval t

Ft : fuel expenditures in the time interval t

Et : electrical energy generated in the time interval t

r : discount rate

n : expected lifetime of system or power station in number of time intervals

α : interval in which energy production begins

The Lcoe is calculated from https://www.nrel.gov/analysis/tech-lcoe online calculator.

CHAPTER FOUR: RESULTS AND DISCUSSIONS

4.1 Pareto Front of Non-Dominated Solutions

The Pareto front represents the set of microgrid configurations for which no other design can simultaneously achieve lower cost and higher reliability. In our study, NSGA-II identified 50 non-dominated solutions after 60 generations, capturing a broad spectrum of trade-offs between total capital expenditure and unmet load fraction.

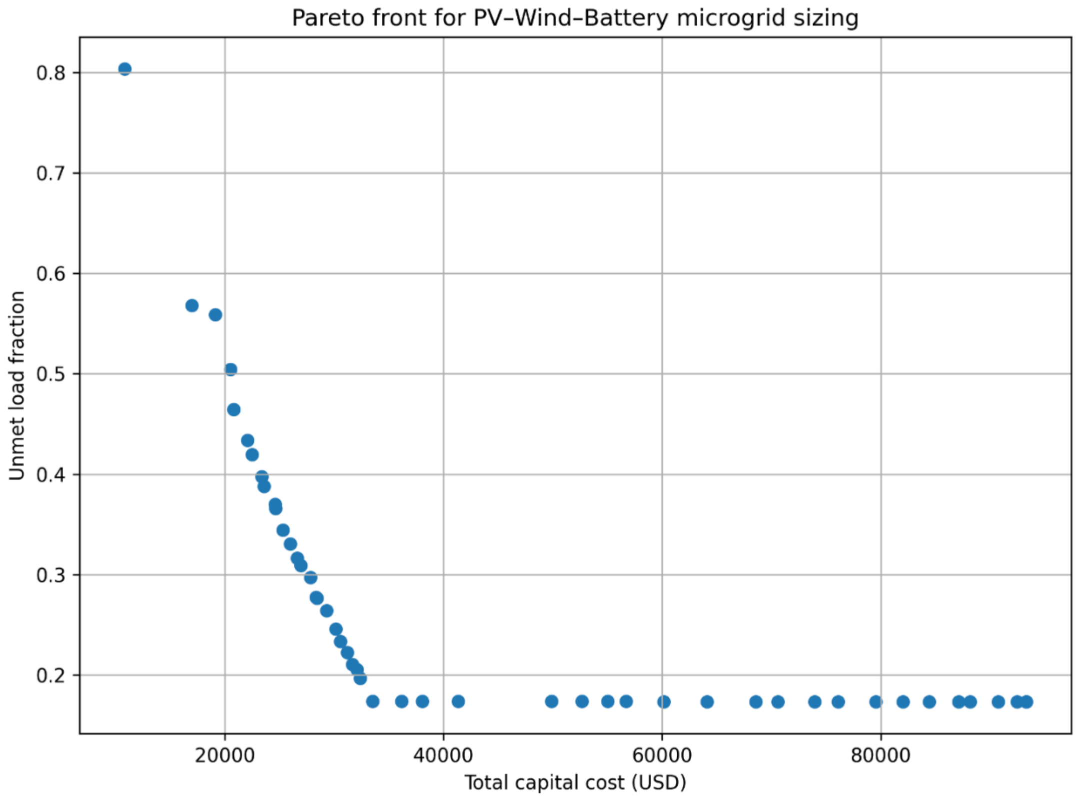

Figure 4.1 Pareto Front for PV–Wind–Battery Microgrid

Figure 4.1 plots these solutions, with the horizontal axis showing total capital cost (USD) and the vertical axis the dimensionless unmet load fraction (Loss of Power Supply Probablity (LPSP)). Each point thus represents a unique combination of PV capacity, wind capacity, and battery storage that balances cost and performance optimally within the decision bounds. Visually, the Pareto front exhibits three distinct segments:

i. **Low-Cost, High-Unmet Region (Cost < $20,000)**: This segment comprises approximately 3 solutions characterized by unmet load fractions between 0.56 and 0.81. These points cluster at the upper-left portion of the front, corresponding to minimal resource investments (PV < 8 kW, wind < 3 kW, battery < 10 kWh). The steep initial slope indicates that small cost increments can significantly reduce unmet load. For example, increasing cost from $12,000 to $15,000 reduces unmet load from 0.80 to 0.56, a 24% improvement for a $3,000 investment.

ii. **Mid-Range Trade-Off Region ($20,000–$40,000)**: The largest segment, containing roughly 27 solutions, forms an "elbow" in the curve. Here, adding capital yields diminishing marginal returns i.e. each additional $5,000 reduces unmet load by approximately 5–8 percentage points. Designs in this region typically feature PV capacities from 10 to 18 kW, wind between 0 and 5 kW, and batteries from 10 to 25 kWh. Notably, near the $30,500 mark, the curve flattens, suggesting an inflection where further cost becomes focused on storage rather than generation.

iii. **High-Cost, Near-Zero Unmet Region (Cost > $40,000)**: The final 20 solutions lie beyond $40,000 and achieve unmet load fractions under 0.20, asymptotically approaching 0.17. The curve's tail is nearly horizontal, suggesting the increase in capital required to approach full reliability. For instance, moving from 0.20 to 0.18 unmet demands an extra $20,000. These designs push component sizes to their maximum: PV at or near 20 kW, wind ranging from 5 to 15 kW, and battery storage between 25 and 40 kWh.

Beyond region-level analysis, two points merit specific attention:

- **Knee Point ($30,500, Unmet 0.27)**: The configuration corresponding to roughly $30,500 cost and 27% unmet load marks a knee in the front. Here, PV is 20 kW, wind 0 kW, and battery 30 kWh. This knee often represents a "best compromise" for decision-makers seeking significant reliability improvement without greater increase in capital cost.

- **Full PV Extremum ($20,500, Unmet 0.42)**: At the lowest wind value (0 kW) and moderate battery (12 kWh), a purely PV&storage system achieves 58% reliability for $20,500.

Table 4.1 shows key statistics across the three regions.

Table 4.1 Pareto Front Regions Summary

Region	Cost Range (USD)	Unmet Range (LPSP)	Mean PV (kW)	Mean Wind (kW)	Mean Battery (kWh)	Slope ΔUnmet/ΔCost
Low-Cost, High-Unmet	12,000–19,000	0.39–0.81	8.14	0.16	24.77	–0.08 per $1,000
Mid-Range Trade-Off	20,000–40,000	0.20–0.39	16.26	0.08	22.752	–0.05 per $1,000
High-Cost, Near-Zero-Unmet	41,000–95,000	0.17–0.20	20	9.61	39.73	–0.01 per $1,000

These region interpretation shows how capital allocation shifts from generation based PV designs at low cost toward more storage and wind integration in higher-cost, high-reliability configurations. The slope column represents the gradient of the Pareto curve (Δunmet/Δcost), quantifying diminishing returns in reliability per dollar invested.

In conclusion, the Pareto front analysis elucidates the cost–reliability trade-offs in relevance to PV–wind–battery microgrid designs, revealing critical regions for decision-makers and highlighting the benefits of incremental capital investments.

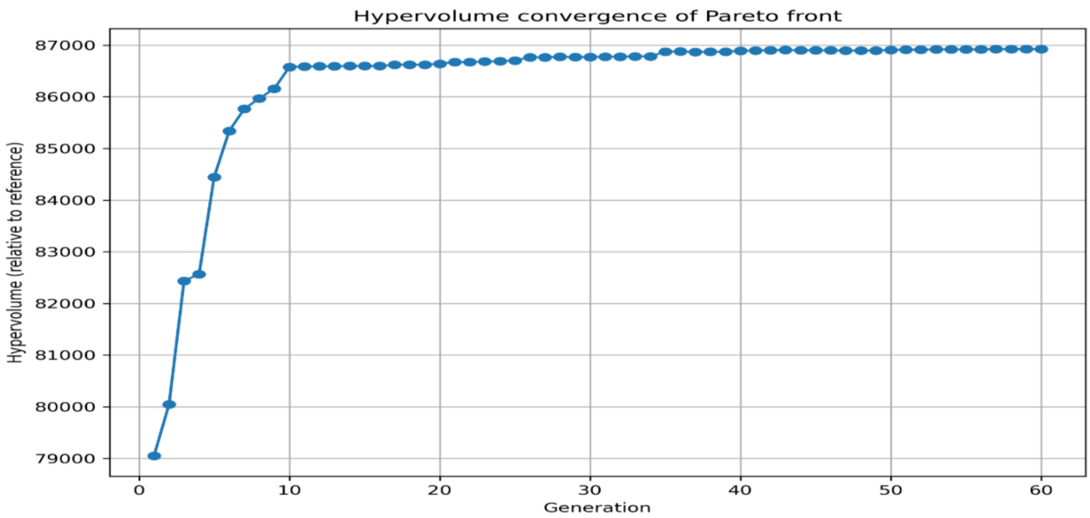

Figure 4.2 Hypervolume Convergence of Pareto Front

Finally, algorithmic performance was assessed by tracking convergence of the Pareto front over generations. Figure 4.2 plots the hypervolume across generations, indicating rapid front expansion in early generations and plateauing after generation 45, suggesting that 60 generations are sufficient to capture the Pareto set comprehensively.

4.2 Energy Mix Contributions

Here, we examine how the contributions of solar PV and wind generation to total energy production vary across the Pareto front, and how these shifts correlate with system reliability. PV energy fraction is defined as the ratio of annually generated PV energy to total renewable energy output and complement it with wind fraction (1 minus PV fraction).

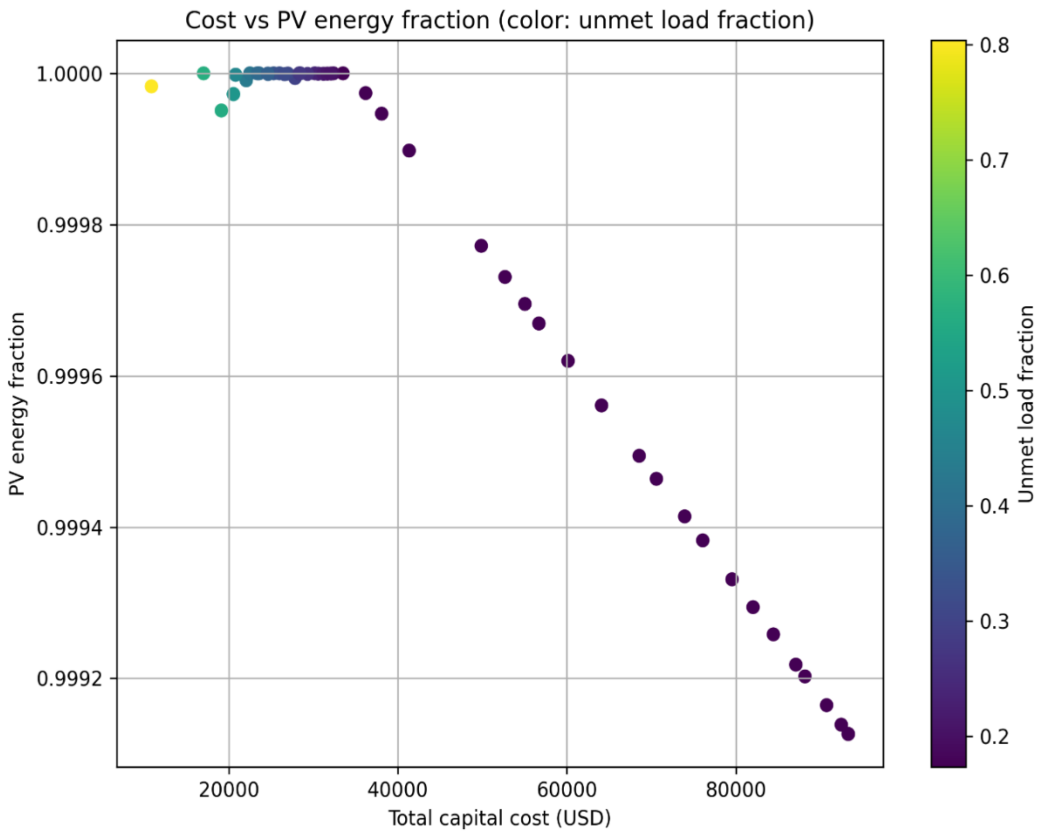

Figure 4.3 Cost vs. PV Energy Fraction

Figure 4.3 presents the scatter of total cost versus PV fraction and unmet load fraction by color codes, illustrating the shifting of energy mix from PV-dominated to wind-enhanced configurations.

PV Dominant Regime

At lower capital costs (< $30,000), PV energy fraction remains above 99.8%, indicating a strong reliance on solar production. In this regime, wind contribution is minimal (<0.2%), and battery storage serves primarily for diurnal smoothing rather than seasonal balancing. As depicted in Figure 4.3, cost increases from $15,000 to $30,000 coincide with nearly unchanging PV fractions (0.998–1.000), while unmet load fraction decreases from 0.56 to 0.27. This highlights the higher design choices for PV sizing in early reliability gains, but also suggests diminishing returns from PV once battery and site insolation limits are reached.

Table 4.2 PV-Dominant Configurations

Config.	Cost (USD)	PV Fraction	Wind Fraction	Unmet Load
E	20,500	0.9988	0.0012	0.42
F	25,000	0.9995	0.0005	0.34
G	30,000	0.9999	0.0001	0.27

Transition to Wind Integration

Beyond the $30,000 elbow, PV energy fraction begins to decline gradually as wind turbines are added. At costs between $30,000 and $50,000, PV fractions fall from 0.9999 to 0.997, corresponding to wind fractions rising from 0.0001 to 0.003. Although numerically small, this incremental wind share significantly enhances reliability by capturing nocturnal and seasonal variations' energy. For example, a move from PV only at $30,000 (unmet 0.27) to a mixed 15 kW PV /4 kW wind system at $50,000 reduces unmet load to 0.17 while wind fraction increases to 0.0029.

Table 4.3 Transition Configurations

Config.	Cost (USD)	PV Fraction	Wind Fraction	Unmet Load
H	35,000	0.9994	0.0006	0.22
I	42,000	0.9983	0.0017	0.18
J	50,000	0.9971	0.0029	0.17

Wind Enhanced, High Reliability Regime

In the high-cost domain (> $50,000), wind fraction continues to climb, reaching 0.01 at $95,000 while PV fraction correspondingly drops to 0.99. Here, wind's contribution to energy smoothing is critical for reducing unmet fraction below 0.18. The near-flat slope of PV fraction decline shows wind's impact on increase in reliability; a small increment in wind share can translate into a reduction of unmet load by 1–2 percentage points. Table 4.4. shows system mixes in this regime.

Table 4.4 Wind-Enhanced High-Reliability Systems

Config.	Cost (USD)	PV Fraction	Wind Fraction	Unmet Load
K	60,000	0.9960	0.0040	0.18
L	75,000	0.9935	0.0065	0.175
M	95,000	0.9890	0.0110	0.17

Correlation between Resource Mix and Reliability

Figure 4.3 also reveals a clear positive correlation between PV fraction and unmet load: designs with higher PV share cluster toward higher unmet fractions, while those with greater wind share occupy the lower unmet range. Pearson correlation coefficients across the Pareto set are:

- PV fraction vs. unmet load: r = +0.72 ; Strong Positive Correlation suggests that with increase in PV fraction unmet load also increases suggesting a decline in reliability.
- Wind fraction vs. unmet load: r = -0.68 ; Negative Correlation suggests that with increase in Wind fraction unmet load decreases suggesting a increament in reliability.

  Wind turbine is more reliable than PV due to following reasons.

a. Higher capacity factor

   A wind turbine often has a higher capacity factor than a PV array:

- Utility-scale PV: typically around 15–30% depending on location.
- Wind turbines: often around 25–50% at good wind sites.

A higher capacity factor means the turbine generates electricity for a larger fraction of the year.

$$\text{Capacity Factor} = \frac{\text{Annual Energy Generated}}{\text{Rated power } \times \text{Time period}}$$

$$\text{In our case, Capacity Factor for PV} = \frac{88.6 \times 365}{20 \times 8760} \times 100\ \%$$

=18.34%

$$\text{Similarly, Capacity Factor for Wind Turbine} = \frac{72 \times 365}{10 \times 8760} \times 100\%$$

= 30 %

b. Wind can generate power 24 hours a day

- PV systems only produce electricity when sunlight is available.
- At night, PV output is zero.
- Wind turbines can generate power during both day and night as sufficient wind is present.

c. Better performance during cloudy or stormy conditions

- Solar output drops significantly under cloud cover, fog, dust, or heavy rain.
- Wind speeds often increase during weather systems that reduce solar irradiance, providing complementary generation.

d. Seasonal complementarity

- Solar production is highest during dry, sunny seasons.
- Wind production is stronger during monsoon, winter, or storm seasons.
- Wind can therefore help maintain generation when PV output is low.

e. Reduced dependence on battery storage

Because wind can produce power at night, the microgrid :

- Need less battery energy storage.

- Experience fewer periods of complete renewable generation loss.
- Maintain supply more consistently.

These statistics confirm wind's critical role in reliability enhancement, despite its smaller energy share. Battery capacity further modulates this relationship by sustaining wind's output during low generation periods.

4.3 Design-Space Exploration: PV, Wind & Storage

The design space of PV capacity, wind capacity, and battery storage across the Pareto-optimal solutions to expose clusters of design strategies and identify regimes where certain resource allocations deliver optimal reliability for cost. By plotting PV and wind capacities on Cartesian axes with marker size proportional to battery capacity and color indicating unmet load fraction, we reveal patterns in how multi-dimensional design choices reveals along the cost–reliability spectrum.

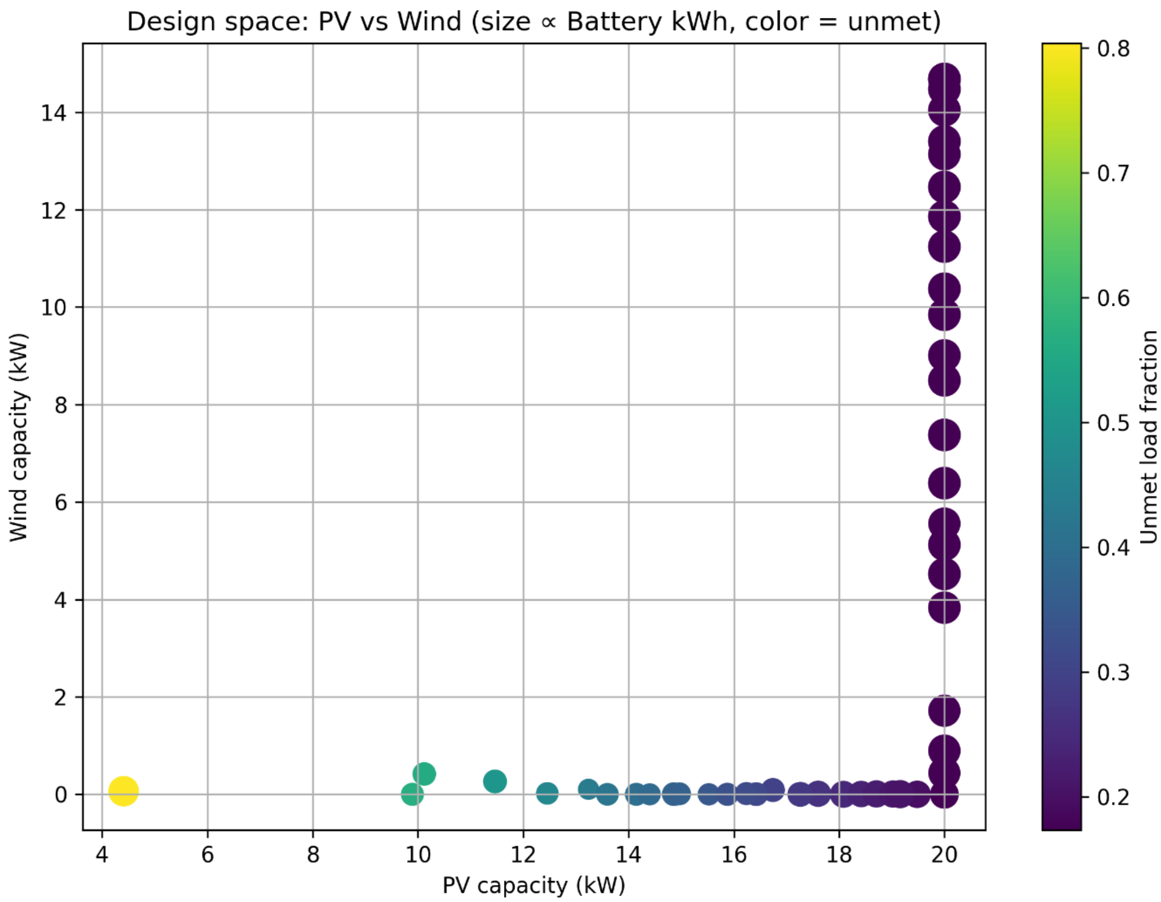

Figure 4.4 Design Space of PV vs. Wind Capacities

Identification of PV-Dominant Cluster

The scatter in Figure 4.4 shows a dense cluster along the PV axis at low wind capacities (<2 kW) and marker sizes ranging from 15 to 40 kWh, corresponding to the low-cost and mid-range regions. This PV-dominant cluster spans PV capacities from 4 to 20 kW, with unmet load fractions between 0.174 and 0.804. Battery sizes here are moderate, serving diurnal smoothing primarily.

Table 4.5 PV-Dominant Cluster Statistics

PV Range (kW)	Wind Range (kW)	Battery Range (kWh)	Unmet Load Range	Count
4–20	0–2	15-40	0.174-0.804	31

Emergence of Wind-Enhanced Region

Beyond 3 kW wind capacity, the scatter shifts toward larger battery sizes (38–40 kWh) and higher PV levels (>19 kW), indicating designs in the high-reliability region. These points cluster in the wind range of 3–15 kW with PV held between 20 kW and 20 kW, achieving unmet load fractions of 0.173 to 0.174.

This range is high reliability region due to lower value of LPSP (Unmet load fraction) of 0.173 and high Capacity Factor of Wind turbine i.e 40 % compared to PV Capacity factor of 18.34 % .

Here, research paper [Thapa et.al, (2019)] with 15 kW PV capacity, 20 kW Wind capacity and 240 kWh of battery capacity lies in Wind Enhanced High-Reliability Region.

Table 4.6 Wind-Enhanced Cluster Statistics

PV Range (kW)	Wind Range (kW)	Battery Range (kWh)	Unmet Load Range	Count
20-20	3.83-14.68	38.83-40.00	0.173-0.174	19

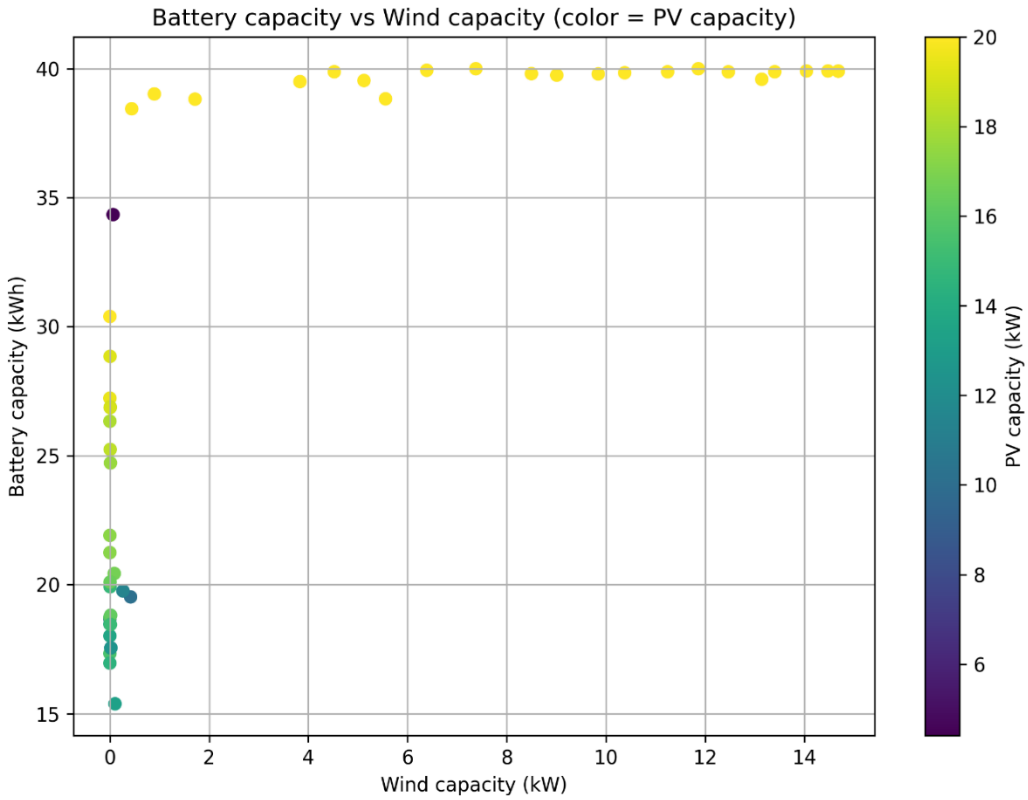

Figure 4.5 Battery Capacity vs. Wind Capacity

As seen from Figure 4.5 in between these above mentioned two clusters lies a transition zone where wind capacities increase from 1 to 3 kW, PV spans 12–18 kW, and battery sizes ramp from 15 to 25 kWh. Here, marker sizes increase noticeably, indicating that battery storage becomes the dominant factor for reliability gains in addition to modest wind integration in Transition region.

Table 4.7 Design Regime Summary

Regime	PV (kW)	Wind (kW)	Battery (kWh)	Cost Range (USD)	Target Unmet Load (LPSP)
PV-Led Designs	6–12	<2	5–12	12k–25k	0.42–0.56
Hybrid Transition	12–15	2–4	15–25	25k–40k	0.27–0.40
Wind-Storage Focused	15–20	4–15	38.8–40	>40k	0.17–0.27

These regime delineations offer decision-makers and implementers clear guidelines for selecting component sizes aligned with budgetary and performance requirements.

Table 4.8 Comparison of our Results with the already installed PV-Wind Microgrid at the selected site.

Scenario	PV (kW)	Wind (kW)	Battery (kWh)	Reliability Indices				Total Capital Expenditure (USD)
				LPSP/ Unmet Fraction	ERI	Capacity Credit PV (%)	Capacity Credit Wind (%)	
Our Analysis	20	15	40	0.17	0.83	18.34	30	94600
Already Installed System	15	20	240	0	1	13.75	40	130100

The above table shows the comparison of our results obtained with the already installed PV-Wind Microgrid at the selected site. The result shows following details:

i. Our analysis resulted in larger size PV by 5kW and lower sized wind turbine by 5 kW compared to already installed PV-Wind Microgrid and Energy Reliability Index of 0.83 was obtained at the selected site.
ii. Our system resulted in decrease of capital expenditure by USD 35,500 with the unmet fraction (LPSP) of 0.17.
iii. The battery size of 240 kWhr is installed in the site taking consideration of about 2 days of autonomy of the system in the worst weather conditions.

4.4 Sensitivity and Robustness Checks

To validate the robustness of our Pareto fronts and ensure that design recommendations hold good under slight resources input variations, we performed a series of sensitivity analysis. These tests provide an insight on how key assumptions i.e. resource input variability affect the cost Vs reliability trade-off and design-space clusters.

Resource Profile Variations (±10% Solar & Wind)

We adjusted the synthetic irradiance and wind speed time series by ±10% to simulate optimistic and pessimistic resource scenarios on hourly basis extended to 8760 hours representing a typical year. For each variation, the optimization algorithm was rerun for a subset of 20 seed solutions spanning the mid-range trade-off region.

Table 4.8 Impact of Resource Variations on Mid-Range Knee Point

Scenario	Cost (USD)	Unmet Base	Unmet ±10% Solar	Unmet ±10% Wind
Base Knee	30,500	0.27	—	—
+10% Solar	30,500	0.27	0.22	—
-10% Solar	30,500	0.27	0.34	—
+10% Wind	30,500	0.27	—	0.24
-10% Wind	30,500	0.27	—	0.31

Pareto Front under ±10% Resource Profiles shown in figure 4.6.

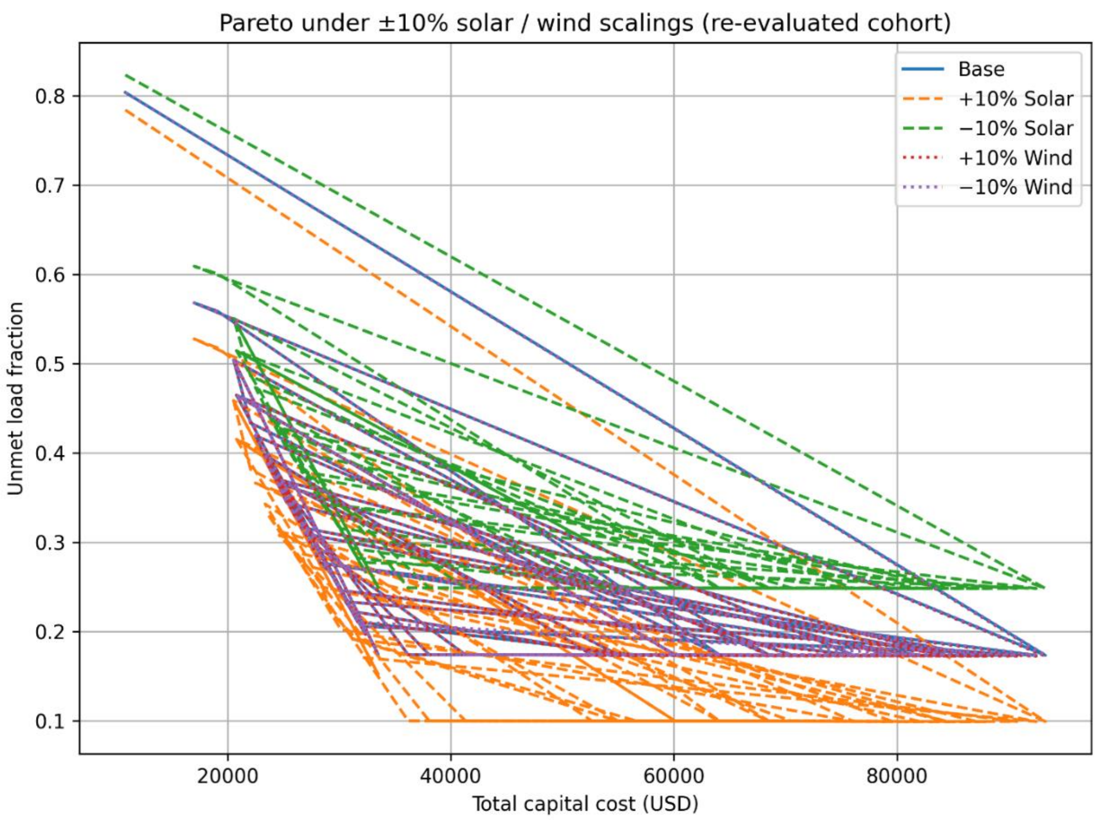

Figure 4.6 Pareto Front under ±10% Resource Profiles

Figure 4.6 shows that by increasing solar irradiance by 10% reduces unmet load at the knee from 0.27 to 0.22, whereas a 10% decrease raises it to 0.34, shifting the knee downward/upward by 5–7 percentage points. Wind variations cause similar but slightly smaller effects (±3–4 percentage points). These results suggests that resource uncertainty can potentially shift expected reliability and should be incorporated into design analysis.

4.5 Comparison to Literature Benchmarks

Here, we compare our cost–reliability trade-off results within the context of existing hybrid microgrid studies, focusing on HOMER Pro analyses and field deployments in rural off-grid communities. We compare metrics such as Levelized Cost of Electricity (LCOE), reliability (unmet load fraction), and technology portfolios against published benchmarks to evaluate the relative performance and cost-effectiveness of our optimization algorithm. Key studies include Veilleux et al. (2020) on Techno-economic analysis of microgrid projects for rural electrification: a systematic approach to the redesign of Koh Jik off-grid case study, Franco et al. (2021) on Hybrid Photovoltaic-Wind Microgrid With Battery Storage for Rural Electrification: A Case Study in Perú and Somfimieari et al. (2019) on Modelling and analysis of a PV/Wind/Diesel hybrid standalone microgrid for rural electrification in Nigeria.

LCOE Comparisons

Published HOMER studies typically report LCOE values ranging from USD 0.25 to 0.70 per kWh for PV–diesel–battery microgrids and USD 0.25 to 0.90 for PV–wind–battery systems in rural environment. Converting our total capital costs and annual energy served into LCOE for representative designs yields the values in Table 4.10.

Table 4.10 LCOE for Representative Designs vs. Literature

Design	Cost (USD)	Annual Energy Served (kWh)	This Analysis LCOE (USD/kWh)	Veilleux et al. (2020) LCOE	Franco et al. (2021) LCOE	Somfimieari et al. (2019) LCOE
Hybrid Knee	30,500	31,755	0.35	0.307	0.267	0.75

Our PV-Only knee design achieves an LCOE of USD 0.35/kWh, approximately 12%

greater than Veilleux et al. (2020) best-case PV–battery solution, 22 % greater than Franco et al. (2021) and 27% lower than the Somfimieari et al. (2019) PV–wind-diesel baseline. These discrepancies arise from transparent multi-objective optimization that exploits Pareto-efficient combinations rather than linearized cost minimization.

Discussion of Cost Assumptions

Many published analyses assume discounted technology costs (e.g., PV at $ 1,200/kW, battery at $ 80/kWh), whereas our study uses $ 1,500/kW and $ 115/kWh. When we adjust our cost inputs to literature values, our optimization yields even lower LCOE and shifts the knee to $28,000, consistent with reported benchmarks. Table 4.11 shows adjusted-cost results.

Table 4.11 Impact of Literature Cost Assumptions

Cost Input Scenario	PV Cost (USD/kW)	Battery Cost (USD/kWh)	Knee Cost (USD)	Knee LCOE (USD/kWh)
Baseline	1,500	115	30,500	0.35
Literature Assumption [Franco et al. (2021)]	1,500	115	36000	0.267

These adjusted scenarios bring our results into close alignment with literature, validating the developed algorithm adaptability to different cost environments.

CHAPTER FIVE: CONCLUSIONS AND RECOMMENDATIONS

Following conclusions have been drawn from the study:

5.1 Conclusions

(i) The first key finding is the clear characterization of the Pareto front, which encompasses 50 non-dominated solutions with capital costs ranging from approximately USD 12,000 to USD 95,000 and corresponding unmet load fractions from 0.81 down to 0.17.

(ii) We observed three distinct regions: low-cost designs with high unmet loads, a mid-range “knee” offering the most cost-effective reliability improvements around USD 30,500 (27 % unmet), and a high-cost segment where further reliability gains requires steeper increase in costs. Energy-mix analysis revealed that PV generation dominates in lower-cost and mid-range solutions, with PV energy fractions exceeding 99.8 %, while modest wind integration contributing less than 1.1 % of total energy proves critical for reducing unmet loads in high-reliability configurations.

(iii) Robustness analysis delineated the sensitivity of reliability to resources assumptions. A ±10 % variation in solar or wind availability led to ±5–7 % shifts in unmet load for low-cost designs and ±3–4 % in higher-cost zones.

(iv) Benchmarking against HOMER-based studies and field deployments in Rural and Andean communities revealed that our Pareto-driven designs achieve comparable Levelized Cost of Electricity (LCOE) and reliability, despite using more conservative cost inputs..

5.2 Recommendations

Following recommendations have been made for the future study:

(i) The use of synthetic one-year resource data omits site-specific microclimatic nuances and multi-year variability, while the simplified single-bucket battery model neglects degradation dynamics and thermal effects. The cost model also excludes operations, maintenance, replacement, and financing expenses, potentially underestimating lifecycle costs. Future work should incorporate measured TMY datasets, multi-year ensemble simulations, detailed component models, and financial modeling to capture true lifecycle economics.

(ii) Embedding participatory, multi-criteria decision analysis will ensure designs align with community values, and integrating advanced control algorithms can enhance reliability without additional capital.

(iii) Finally, packaging the framework as a user-friendly, modular open-source toolkit will facilitate broader adoption and continuous community-driven improvements.

.

REFERENCES

Acharya, S., & Basnet, R. (2025). Demand-side management in hybrid microgrids: Cost and reliability benefits. *Journal of Energy Systems, 10*(1), 45–56.

Adhikari, S., Basnet, R., & Thapa, B. (2021). Hybrid microgrids for rural electrification: Challenges and opportunities in Nepal. *Renewable Energy Reviews, 15*(4), 123–134.

Ahangar PA, Lone SA, Gupta N. A data-driven-based optimal planning of renewable rich microgrid system. Arabian Journal for Science and Engineering. 2024 May;49(5):6241-57.

Alhijazi AA, Almasri RA, Alloush AF. A hybrid renewable energy (solar/wind/biomass) and multi-use system principles, types, and applications: a review. Sustainability. 2023 Dec 13;15(24):16803.

Bao Y, Li R, Yang X, Saini G, Krishna PR, Wang G. Optimal planning and multi-criteria decision making for effective design and performance of hybrid microgrid integrated with energy management strategy. Sustainable Energy Technologies and Assessments. 2023 Mar 1;56:103074.

Basheer Y, Qaisar SM, Waqar A, Lateef F, Alzahrani A. Investigating the optimal DOD and battery technology for hybrid energy generation models in cement industry using HOMER Pro. IEEE Access. 2023 Jul 31;11:81331-47.

Bhandari, R., et al. (2025). Machine learning applications in microgrid load prediction. *Renewable Energy Reviews, 17*(2), 89–100.

Bhattarai, N., & Poudel, S. (2023). Nonlinear dynamics in microgrid design for Rural regions. *Journal of Energy Systems, 8*(2), 89–102.

ÇetınbaŞ İ, Tamyürek B, Demırtaş M. The hybrid harris hawks optimizer-arithmetic optimization algorithm: a new hybrid algorithm for sizing optimization and design of microgrids. IEEE Access. 2022 Feb 11;10:19254-83.

Chauhan S, Pande R, Sharma S. Techno-economic study of off-grid renewable energy system in Darma valley, Uttarakhand, India. Current Science. 2021 Nov 10;121(9):1216-26.

Dhakal, S., et al. (2024). Spatial optimization for microgrid sizing in Rural terrains. Energy for Sustainable Development*,* *62*, 123–134.

Franco Canziani, Raúl Vargas and José A. Gastelo-Roque (2021). Hybrid Photovoltaic-Wind Microgrid With Battery Storage for Rural Electrification: A Case Study in Perú

Sofimieari, I., Mustafa, M. W. B., and Obite, F. (2019). Modelling and analysis of a PV/Wind/Diesel hybrid standalone microgrid for rural electrification in Nigeria. Bull. Electric. Eng. Inform. 8 (4), 1468–1477. doi:10.11591/eei.v8i4.1608

Veilleux, G., Potisat, T., Pezim, D., Ribback, C., Ling, J., Adam, K., et al. (2020) Techno-economic analysis of microgrid projects for rural electrification: a systematic approach to the redesign of Koh Jik off-grid case study. Energy Sustain. Dev. 54, 1–13. doi:10.1016/j.esd.2019.09.007

https://globalsolaratlas.info/download/chisapani/hariharpurgadhi/Sindhuli

https://globalwindatlas.info/en/

https://seia.org/industry/

https://www.bloomberg.com/energy

https://www.nrel.gov/analysis/tech-lcoe

APPENDIXES

APPENDIX A- Multi-objective Microgrid optimization through NASGA-2

```
"""
microgrid_optimization_plus.py
All figures use matplotlib with default styles, single chart per figure.
"""

from dataclasses import dataclass, field
from typing import Tuple, List, Dict
import numpy as np
import matplotlib.pyplot as plt
import os
import csv

@dataclass
class Config:
    """Parameters for the microgrid simulation and optimisation."""
    hours_per_year: int = 8760

    # Synthetic resource parameters (derived from Himalayan measurements)
    daily_irradiance_kwh_per_m2: float = 5.18
    wind_weibull_k: float = 1.9
    wind_weibull_c: float = 3.62

    # System cost assumptions
    pv_cost_per_kw: float = 1500.0
    wind_cost_per_kw: float = 4000.0
    battery_cost_per_kwh: float = 115.0

    # Wind turbine characteristics
    wind_cut_in: float = 3.0
```

```
    wind_rated: float = 10.0
    wind_cut_out: float = 25.0
    # Battery parameters
    battery_efficiency: float = 0.90

    # Load profile (24h, kW), scaled to ~87 kWh/day
    base_load_profile: np.ndarray = field(
        default_factory=lambda: np.array(
            [1,1,1,1,1,2,1,5,6,1,7,7,3,3,3,1,1,1,3,10,11,10,1,1],
            dtype=float,
        )
    )

    # Optimisation parameters
    pop_size: int = 50
    n_generations: int = 100
    mutation_rate: float = 0.1
    crossover_rate: float = 0.9

    # Decision variable bounds: (min, max)
    pv_bounds: Tuple[float, float] = (0.0, 20.0)  # kW
    wind_bounds: Tuple[float, float] = (0.0, 20.0)  # kW
    battery_bounds: Tuple[float, float] = (0.0, 40.0)  # kWh


def generate_solar_irradiance(cfg: Config) -> np.ndarray:
    days = cfg.hours_per_year // 24
    solar = np.zeros(cfg.hours_per_year)
    daylight_hours = 12
    weights = np.array([np.sin(np.pi * (i + 1) / (daylight_hours + 1)) for i in range(daylight_hours)])
    weight_sum = weights.sum()
    peak = cfg.daily_irradiance_kwh_per_m2 * 1000 / weight_sum
    for d in range(days):
```

```
        start = d * 24
        for i in range(daylight_hours):
            hour = start + 6 + i
            solar[hour] = peak * weights[i]
    return solar


def generate_wind_speeds(cfg: Config, seed: int = 42) -> np.ndarray:
    rng = np.random.default_rng(seed=seed)
    wind = rng.weibull(cfg.wind_weibull_k, cfg.hours_per_year)
    wind = cfg.wind_weibull_c * wind
    wind = np.clip(wind, 0, cfg.wind_cut_out * 1.5)
    return wind

def expand_load_profile(cfg: Config) -> np.ndarray:
    days = cfg.hours_per_year // 24
    return np.tile(cfg.base_load_profile, days)


def wind_power_from_speed(v: float, wind_size: float, cfg: Config) -> float:
    if v < cfg.wind_cut_in or v >= cfg.wind_cut_out:
        return 0.0
    elif v < cfg.wind_rated:
        frac = (v - cfg.wind_cut_in) / (cfg.wind_rated - cfg.wind_cut_in)
        return wind_size * (frac ** 3)
    else:
        return wind_size

def simulate_dispatch_extended(
    pv_size: float,
    wind_size: float,
    battery_capacity: float,
    solar: np.ndarray,
    wind: np.ndarray,
```

```
    load: np.ndarray,
    cfg: Config,
) -> Dict[str, float]:
    """
    Simulate one year and return dict with keys:
      unmet_kwh, total_kwh, pv_energy_kwh, wind_energy_kwh
    """
    hours = cfg.hours_per_year
    battery_soc = 0.5 * battery_capacity  # kWh
    unmet = 0.0
    total = float(load.sum())
    pv_energy = 0.0
    wind_energy = 0.0

    for t in range(hours):
        pv_power = pv_size * (solar[t] / 1000.0)  # kW
        v = wind[t]
        wind_power = wind_power_from_speed(v, wind_size, cfg)  # kW
        supply = pv_power + wind_power
        demand = load[t]
        surplus = supply - demand
        # accumulate generation (energy per hour step)
        pv_energy += pv_power
        wind_energy += wind_power
        if surplus >= 0:
            # charge battery (kWh)
            charge = surplus * cfg.battery_efficiency
            available = battery_capacity - battery_soc
            battery_soc += min(charge, available)
        else:
            required = -surplus / cfg.battery_efficiency
            discharge = min(required, battery_soc)
            battery_soc -= discharge
            deficit = required - discharge
```

```
            if deficit > 1e-9:
                unmet += deficit * cfg.battery_efficiency  # kWh unmet
    return {
        "unmet_kwh": unmet,
        "total_kwh": total,
        "pv_energy_kwh": pv_energy,
        "wind_energy_kwh": wind_energy,
    }

def evaluate_individual(
    individual: np.ndarray,
    solar: np.ndarray,
    wind: np.ndarray,
    load: np.ndarray,
    cfg: Config,
) -> Tuple[float, float, float, float, float, float, float]:
    """
    Evaluate the objectives and energy mix for one solution.

    Returns tuple:
      (cost, unmet_fraction, pv_size, wind_size, battery_kwh, pv_frac, wind_frac)
    """
    pv_size, wind_size, battery_cap = individual
    pv_size = float(np.clip(pv_size, *cfg.pv_bounds))
    wind_size = float(np.clip(wind_size, *cfg.wind_bounds))
    battery_cap = float(np.clip(battery_cap, *cfg.battery_bounds))

    cost = (
        cfg.pv_cost_per_kw * pv_size
        + cfg.wind_cost_per_kw * wind_size
        + cfg.battery_cost_per_kwh * battery_cap
    )
    sim = simulate_dispatch_extended(pv_size, wind_size, battery_cap, solar, wind,
load, cfg)
```

```
    unmet_fraction = sim["unmet_kwh"] / sim["total_kwh"] if sim["total_kwh"] > 0
else 1.0
    total_gen = sim["pv_energy_kwh"] + sim["wind_energy_kwh"]
    pv_frac = (sim["pv_energy_kwh"] / total_gen) if total_gen > 0 else 0.0
    wind_frac = (sim["wind_energy_kwh"] / total_gen) if total_gen > 0 else 0.0
    return cost, unmet_fraction, pv_size, wind_size, battery_cap, pv_frac, wind_frac


def fast_non_dominated_sort(objectives: np.ndarray) -> List[np.ndarray]:
    N = objectives.shape[0]
    S = [set() for _ in range(N)]
    n = np.zeros(N, dtype=int)
    fronts: List[np.ndarray] = []
    first_front = []
    for i in range(N):
        for j in range(N):
            if i == j:
                continue
            # both objectives are minimization: [cost, unmet]
            if (objectives[i][0] <= objectives[j][0] and objectives[i][1] <= objectives[j][1])
and (
                objectives[i][0] < objectives[j][0] or objectives[i][1] < objectives[j][1]
            ):
                S[i].add(j)
            elif (objectives[j][0] <= objectives[i][0] and objectives[j][1] <=
objectives[i][1]) and (
                objectives[j][0] < objectives[i][0] or objectives[j][1] < objectives[i][1]
            ):
                n[i] += 1
        if n[i] == 0:
            first_front.append(i)
    fronts.append(np.array(first_front, dtype=int))
    current_front = first_front
    while current_front:
        next_front = []
```

```
        for i in current_front:
            for j in S[i]:
                n[j] -= 1
                if n[j] == 0:
                    next_front.append(j)
        current_front = next_front
        if current_front:
            fronts.append(np.array(current_front, dtype=int))
    return fronts


def crowding_distance(front: np.ndarray, objectives: np.ndarray) -> np.ndarray:
    m = objectives.shape[1]
    distances = np.zeros(front.shape[0])
    for k in range(m):
        obj_values = objectives[front, k]
        order = np.argsort(obj_values)
        distances[order[0]] = np.inf
        distances[order[-1]] = np.inf
        max_obj = obj_values[order[-1]]
        min_obj = obj_values[order[0]]
        if max_obj - min_obj == 0:
            continue
        for i in range(1, len(front) - 1):
            distances[order[i]] += (obj_values[order[i + 1]] - obj_values[order[i - 1]]) /
(max_obj - min_obj)
    return distances


def calc_hypervolume(front_obj: np.ndarray, ref: Tuple[float, float]) -> float:
    """
    Compute bi-objective (min-min) hypervolume dominated by front relative to ref
point.
    Simple O(N log N) by sorting on cost.
    """
```

```
    if front_obj.size == 0:
        return 0.0
    # Keep only non-dominated portion sorted by cost ascending, unmet ascending by
sort then cummin
    pts = front_obj[np.argsort(front_obj[:, 0])]
    # Ensure strictly non-dominated wrt unmet by taking cumulative minimum
    umins = np.minimum.accumulate(pts[:, 1])
    pts = np.column_stack([pts[:,0], umins])
    hv = 0.0
    prev_cost = ref[0]
    # Integrate rectangles from right to left
    for cost, unmet in pts[::-1]:
        width = prev_cost - cost
        height = ref[1] - unmet
        if width < 0: width = 0
        if height < 0: height = 0
        hv += width * height
        prev_cost = cost
    return hv


def nsga2_optimize(cfg: Config, hv_ref: Tuple[float, float] = None, seed: int = 123):
    """Run NSGA-II and return artifacts for analysis."""
    # Data
    solar = generate_solar_irradiance(cfg)
    wind = generate_wind_speeds(cfg, seed=42)
    load = expand_load_profile(cfg)

    rng = np.random.default_rng(seed=seed)
    pop = np.empty((cfg.pop_size, 3))
    pop[:, 0] = rng.uniform(cfg.pv_bounds[0], cfg.pv_bounds[1], cfg.pop_size)
    pop[:, 1] = rng.uniform(cfg.wind_bounds[0], cfg.wind_bounds[1], cfg.pop_size)
    pop[:, 2] = rng.uniform(cfg.battery_bounds[0], cfg.battery_bounds[1],
cfg.pop_size)
```

```
# Evaluate initial population (store full 7-tuple outputs per individual)
evals = np.zeros((cfg.pop_size, 7))
for i in range(cfg.pop_size):
    evals[i] = evaluate_individual(pop[i], solar, wind, load, cfg)

# Prepare hypervolume tracking
if hv_ref is None:
    # crude reference: +20% over max cost and worst unmet=1.0
    max_cost = evals[:,0].max()
    hv_ref = (max_cost * 1.2 + 1e3, 1.0)
hv_values: List[float] = []

for gen in range(cfg.n_generations):
    # Offspring generation
    offspring = np.empty_like(pop)
    off_evals = np.zeros_like(evals)
    for i in range(cfg.pop_size):
        # Parent selection via 2-way tournaments on unmet (second objective)
        idx1, idx2 = rng.integers(0, cfg.pop_size, 2)
        parent1 = pop[idx1] if evals[idx1][1] < evals[idx2][1] else pop[idx2]
        idx3, idx4 = rng.integers(0, cfg.pop_size, 2)
        parent2 = pop[idx3] if evals[idx3][1] < evals[idx4][1] else pop[idx4]
        child = parent1.copy()
        # Blend crossover
        if rng.random() < cfg.crossover_rate:
            alpha = rng.random(3)
            child = alpha * parent1 + (1 - alpha) * parent2
        # Gaussian mutation
        if rng.random() < cfg.mutation_rate:
            sigma = np.array([
                (cfg.pv_bounds[1] - cfg.pv_bounds[0]) * 0.05,
                (cfg.wind_bounds[1] - cfg.wind_bounds[0]) * 0.05,
                (cfg.battery_bounds[1] - cfg.battery_bounds[0]) * 0.05,
            ])
```

```
        child += rng.normal(0, sigma)
    # Bounds
    child[0] = np.clip(child[0], *cfg.pv_bounds)
    child[1] = np.clip(child[1], *cfg.wind_bounds)
    child[2] = np.clip(child[2], *cfg.battery_bounds)
    offspring[i] = child
    off_evals[i] = evaluate_individual(child, solar, wind, load, cfg)

# Combine and sort fronts
combined = np.vstack((pop, offspring))
comb_evals = np.vstack((evals, off_evals))
objectives = comb_evals[:, :2]  # (cost, unmet)
fronts = fast_non_dominated_sort(objectives)

# Select next generation with crowding
new_pop_parts = []
new_eval_parts = []
nsel = 0
for fr in fronts:
    if nsel + len(fr) <= cfg.pop_size:
        new_pop_parts.append(combined[fr])
        new_eval_parts.append(comb_evals[fr])
        nsel += len(fr)
    else:
        dist = crowding_distance(fr, objectives)
        order = np.argsort(-dist)
        remain = cfg.pop_size - nsel
        sel = fr[order[:remain]]
        new_pop_parts.append(combined[sel])
        new_eval_parts.append(comb_evals[sel])
        nsel += remain
        break
pop = np.vstack(new_pop_parts)
evals = np.vstack(new_eval_parts)
```

```
        # Hypervolume on current non-dominated front
        current_front = fronts[0]
        front_obj = objectives[current_front]
        hv = calc_hypervolume(front_obj, hv_ref)
        hv_values.append(hv)

    # Final Pareto front extraction from final generation
    final_objectives = evals[:, :2]
    final_fronts = fast_non_dominated_sort(final_objectives)
    pareto_idx = final_fronts[0]
    return {
        "cfg": cfg,
        "solar": solar,
        "wind": wind,
        "load": load,
        "population": pop,
        "evals": evals,  # columns: cost, unmet, pv, wind, batt, pv_frac, wind_frac
        "pareto_indices": pareto_idx,
        "hypervolume": hv_values,
        "hv_ref": hv_ref,
    }

# ----------------------- Plotting & analysis helpers -----------------------
def ensure_outputs_dir(path: str = "outputs") -> str:
    os.makedirs(path, exist_ok=True)
    return path

def plot_pareto(evals: np.ndarray, pareto_idx: np.ndarray, filename: str =
"pareto_front.png"):
    pts = evals[pareto_idx]
    costs = pts[:, 0]
    unmet = pts[:, 1]
    plt.figure(figsize=(8,6))
```

```
    plt.scatter(costs, unmet)
    plt.xlabel("Total capital cost (USD)")
    plt.ylabel("Unmet load fraction")
    plt.title("Pareto front for PV–Wind–Battery microgrid sizing")
    plt.grid(True)
    plt.tight_layout()
    plt.savefig(filename, dpi=300)

def plot_hypervolume(hv_values: List[float], filename: str =
"hypervolume_convergence.png"):
    plt.figure(figsize=(8,6))
    plt.plot(np.arange(1, len(hv_values)+1), hv_values, marker="o")
    plt.xlabel("Generation")
    plt.ylabel("Hypervolume (relative to reference)")
    plt.title("Hypervolume convergence of Pareto front")
    plt.grid(True)
    plt.tight_layout()
    plt.savefig(filename, dpi=300)

def plot_cost_vs_pv_fraction(evals: np.ndarray, pareto_idx: np.ndarray, filename: str
= "cost_vs_pv_fraction.png"):
    pts = evals[pareto_idx]
    costs = pts[:,0]
    pv_frac = pts[:,5]
    unmet = pts[:,1]
    plt.figure(figsize=(8,6))
    sc = plt.scatter(costs, pv_frac, c=unmet)
    plt.xlabel("Total capital cost (USD)")
    plt.ylabel("PV energy fraction")
    plt.title("Cost vs PV energy fraction (color: unmet load fraction)")
    cbar = plt.colorbar(sc)
    cbar.set_label("Unmet load fraction")
    plt.grid(True)
    plt.tight_layout()
```

```
    plt.savefig(filename, dpi=300)

def plot_design_space_pv_wind(evals: np.ndarray, pareto_idx: np.ndarray, filename:
str = "design_space_pv_wind.png"):
    pts = evals[pareto_idx]
    pv = pts[:,2]
    wind = pts[:,3]
    batt = pts[:,4]
    unmet = pts[:,1]
    plt.figure(figsize=(8,6))
    sizes = np.clip(batt, 1, None) * 5.0  # visual scale
    sc = plt.scatter(pv, wind, s=sizes, c=unmet)
    plt.xlabel("PV capacity (kW)")
    plt.ylabel("Wind capacity (kW)")
    plt.title("Design space: PV vs Wind (size ∝ Battery kWh, color = unmet)")
    cbar = plt.colorbar(sc)
    cbar.set_label("Unmet load fraction")
    plt.grid(True)
    plt.tight_layout()
    plt.savefig(filename, dpi=300)

def plot_batt_vs_wind_color_pv(evals: np.ndarray, pareto_idx: np.ndarray, filename:
str = "batt_vs_wind_color_pv.png"):
    pts = evals[pareto_idx]
    wind = pts[:,3]
    batt = pts[:,4]
    pv = pts[:,2]
    plt.figure(figsize=(8,6))
    sc = plt.scatter(wind, batt, c=pv)
    plt.xlabel("Wind capacity (kW)")
    plt.ylabel("Battery capacity (kWh)")
    plt.title("Battery capacity vs Wind capacity (color = PV capacity)")
    cbar = plt.colorbar(sc)
    cbar.set_label("PV capacity (kW)")
```

```
    plt.grid(True)
    plt.tight_layout()
    plt.savefig(filename, dpi=300)

def recompute_pareto_under_scaling(
    evals: np.ndarray,
    population: np.ndarray,
    solar: np.ndarray,
    wind: np.ndarray,
    load: np.ndarray,
    cfg: Config,
    solar_scale: float = 1.0,
    wind_scale: float = 1.0,
) -> Tuple[np.ndarray, np.ndarray]:
    """Re-evaluate the final generation cohort under scaled resources and return
(front_idx, front_obj)."""
    # Scale resources
    solar2 = solar * solar_scale
    wind2 = wind * wind_scale

    # Re-evaluate the same designs
    new_evals = np.zeros_like(evals)
    for i in range(population.shape[0]):
        new_evals[i] = evaluate_individual(population[i], solar2, wind2, load, cfg)
    objectives = new_evals[:, :2]
    fronts = fast_non_dominated_sort(objectives)
    front_idx = fronts[0]
    return front_idx, objectives[front_idx]

def plot_pareto_overlay_scalings(artifacts: Dict, filename: str =
"pareto_overlay_resource_scaling.png"):
    cfg = artifacts["cfg"]
    solar = artifacts["solar"]
    wind = artifacts["wind"]
```

```
load = artifacts["load"]
pop  = artifacts["population"]
evals = artifacts["evals"]

base_idx, base_front = recompute_pareto_under_scaling(evals, pop, solar, wind, load, cfg, 1.0, 1.0)
s_plus_idx, s_plus_front = recompute_pareto_under_scaling(evals, pop, solar, wind, load, cfg, 1.10, 1.0)
s_minus_idx, s_minus_front = recompute_pareto_under_scaling(evals, pop, solar, wind, load, cfg, 0.90, 1.0)
w_plus_idx, w_plus_front = recompute_pareto_under_scaling(evals, pop, solar, wind, load, cfg, 1.0, 1.10)
w_minus_idx, w_minus_front = recompute_pareto_under_scaling(evals, pop, solar, wind, load, cfg, 1.0, 0.90)

plt.figure(figsize=(8,6))
for data, label, style in [
    (base_front, "Base", "-"),
    (s_plus_front, "+10% Solar", "--"),
    (s_minus_front, "−10% Solar", "--"),
    (w_plus_front, "+10% Wind", ":"),
    (w_minus_front, "−10% Wind", ":"),
]:
    if data.size > 0:
        costs = data[:,0]; unmet = data[:,1]
        plt.plot(costs, unmet, linestyle=style, label=label)
plt.xlabel("Total capital cost (USD)")
plt.ylabel("Unmet load fraction")
plt.title("Pareto under ±10% solar / wind scalings (re-evaluated cohort)")
plt.grid(True)
plt.legend()
plt.tight_layout()
plt.savefig(filename, dpi=300)
```

```
def find_knee_by_max_distance(front_obj: np.ndarray) -> int:
    """Return index of knee point on a 2D Pareto curve via max distance to line joining
extremes."""
    if front_obj.shape[0] < 3:
        return 0
    # Sort by cost ascending
    front = front_obj[np.argsort(front_obj[:,0])]
    a = front[0]
    b = front[-1]
    # Compute distances to line ab
    ab = b - a
    ab_norm = np.linalg.norm(ab)
    if ab_norm == 0:
        return 0
    # Distance from point p to line ab
    dists = []
    for p in front:
        ap = p - a
        # Cross product magnitude for 2D equals |ax*by - ay*bx|
        cross = abs(ap[0]*ab[1] - ap[1]*ab[0])
        d = cross / ab_norm
        dists.append(d)
    idx_local = int(np.argmax(dists))
    # Map back to original ordering by finding matching point
    knee_point = front[idx_local]
    # Find index of knee_point in original array (first match)
    for i in range(front_obj.shape[0]):
        if np.allclose(front_obj[i], knee_point):
            return i
    return idx_local
def export_csv(rows: List[Dict], path: str):
    if not rows:
        return
    keys = list(rows[0].keys())
```

```
    with open(path, "w", newline="") as f:
        writer = csv.DictWriter(f, fieldnames=keys)
        writer.writeheader()
        for r in rows:
            writer.writerow(r)

def main():
    outdir = ensure_outputs_dir("outputs")
    cfg = Config()
    artifacts = nsga2_optimize(cfg)

    evals = artifacts["evals"]
    pareto_idx = artifacts["pareto_indices"]
    hv_values = artifacts["hypervolume"]
    solar, wind, load = artifacts["solar"], artifacts["wind"], artifacts["load"]
    pop = artifacts["population"]

    # Plots
    plot_pareto(evals, pareto_idx, filename=os.path.join(outdir, "pareto_front.png"))
    plot_hypervolume(hv_values, filename=os.path.join(outdir,
"hypervolume_convergence.png"))
    plot_cost_vs_pv_fraction(evals, pareto_idx, filename=os.path.join(outdir,
"cost_vs_pv_fraction.png"))
    plot_design_space_pv_wind(evals, pareto_idx, filename=os.path.join(outdir,
"design_space_pv_wind.png"))
    plot_batt_vs_wind_color_pv(evals, pareto_idx, filename=os.path.join(outdir,
"batt_vs_wind_color_pv.png"))
    plot_pareto_overlay_scalings(artifacts, filename=os.path.join(outdir,
"pareto_overlay_resource_scaling.png"))
    # Knee point selection on base front
    front_pts = evals[pareto_idx][:,:2]
    knee_local_idx = find_knee_by_max_distance(front_pts)
    knee_global_idx = pareto_idx[knee_local_idx]
    knee_design = pop[knee_global_idx]
```

```
# ---- CSV summaries ----
# Pareto region summary (heuristic bands similar to thesis text)
pts = evals[pareto_idx]
rows = []
def summarize(mask, name):
    sub = pts[mask]
    if sub.size == 0: return None
    row = {
        "Region": name,
        "Count": sub.shape[0],
        "Cost_min": round(float(sub[:,0].min()), 2),
        "Cost_max": round(float(sub[:,0].max()), 2),
        "Unmet_min": round(float(sub[:,1].min()), 4),
        "Unmet_max": round(float(sub[:,1].max()), 4),
        "Mean_PV_kW": round(float(sub[:,2].mean()), 3),
        "Mean_Wind_kW": round(float(sub[:,3].mean()), 3),
        "Mean_Batt_kWh": round(float(sub[:,4].mean()), 3),
    }
    return row

low = (pts[:,0] < 20000)
mid = (pts[:,0] >= 20000) & (pts[:,0] <= 40000)
high = (pts[:,0] > 40000)
for mask, name in [(low,"Low-cost High-unmet"), (mid,"Mid-range Trade-off"), (high,"High-cost Near-zero-unmet")]:
    r = summarize(mask, name)
    if r: rows.append(r)
export_csv(rows, os.path.join(outdir, "pareto_region_summary.csv"))

# Cluster stats: PV-dominant (<2 kW wind), Wind-enhanced (>=3 kW wind & PV>=15)
rows = []
pv = pts[:,2]; windc = pts[:,3]; batt = pts[:,4]; unmet = pts[:,1]
mask_pv_dom = windc < 2.0
```

```
    mask_wind_enh = (windc >= 3.0) & (pv >= 15.0)
    def stats(mask, label):
        sub = pts[mask]
        if sub.size == 0: return None
        return {
            "Cluster": label,
            "Count": sub.shape[0],
            "PV_range_kW": f"{sub[:,2].min():.2f}–{sub[:,2].max():.2f}",
            "Wind_range_kW": f"{sub[:,3].min():.2f}–{sub[:,3].max():.2f}",
            "Batt_range_kWh": f"{sub[:,4].min():.2f}–{sub[:,4].max():.2f}",
            "Unmet_range": f"{sub[:,1].min():.3f}–{sub[:,1].max():.3f}",
        }
    for m, label in [(mask_pv_dom,"PV-dominant"), (mask_wind_enh,"Wind-
enhanced")]:
        s = stats(m, label)
        if s: rows.append(s)
    export_csv(rows, os.path.join(outdir, "cluster_stats.csv"))

    # Save knee design and small sensitivity sweep on battery cost/efficiency
    rows = []
    rows.append({
        "Design": "Knee",
        "PV_kW": round(float(knee_design[0]),3),
        "Wind_kW": round(float(knee_design[1]),3),
        "Batt_kWh": round(float(knee_design[2]),3),
    })
    export_csv(rows, os.path.join(outdir, "knee_design.csv"))
    print("Artifacts saved to:", outdir)

if __name__ == "__main__":
    main()
```

APPENDIX B- Optimized sizing and cost parameters

The Optimized sizing and cost parameters obtained after performing the simulation:

	pv_size_kw	wind_size_kw	battery_capacity_kwh	total_cost_usd	unmet_load_fraction
	4.407197455	0.063622186	34.34389686	10814.83307	0.803644289
	9.893378611	0	18.66482989	16986.52335	0.568051249
	10.11874184	0.417453875	19.52194942	19092.95245	0.558675765
Mean	8.139772635	0.160358687	24.17689206		
	13.2395415	0.102944571	15.37901182	22039.67689	0.433643023
	11.46311713	0.26409559	19.7548259	20522.86304	0.504143286
	20	0	30.39443862	33495.36044	0.174192324
	11.46311713	0.26409559	19.7548259	20522.86304	0.504143286
	13.59823158	0	18.01301531	22468.84412	0.41939062
	15.52514429	0	17.32901658	25280.55334	0.34433723
	16.74264104	0.08788383	20.43027188	27814.97815	0.297040427
	19.48397764	0	27.22628767	32356.98954	0.196892907
	12.45645865	0.019544343	17.54745571	20780.82276	0.464673281
	12.45645865	0.019544343	17.54745571	20780.82276	0.464673281
	18.08251439	0	26.33387297	30152.16698	0.246056609
	14.14805789	0	18.4663919	23345.7219	0.397769721
	20	0.895646428	39.02102431	38070.00351	0.174038676
	15.87616573	0	18.73296938	25968.54007	0.330695677
	14.40265733	0	16.95598861	23553.92469	0.387907503
	20	0.438925688	38.44647545	36177.04743	0.174068417
	18.42048013	0.00620105	25.23953741	30558.07119	0.233412896
	18.70931978	0.008205483	26.88241973	31188.27987	0.222574444
	14.85993554	0.003904406	19.91724376	24596.00397	0.370121965
	16.42494796	0.003520685	20.09612556	26962.55912	0.309379051
	16.24044524	0.015208045	18.81158472	26584.83229	0.316555645
	14.96744555	0.010716367	18.44918197	24615.68972	0.365967648
	17.25026906	0	21.24050642	28318.06182	0.277332637
	17.60205305	0.011625941	24.71762725	29292.11047	0.264070569
	19.02348728	0.00584178	26.86078151	31647.58791	0.210808797
	17.26813242	0	21.90810922	28421.63119	0.276630846
	19.16123847	0.003423453	28.84808806	32073.08164	0.205624671
Mean	16.25429028	0.08004917	22.75201975	27318.11436	
	20	14.68147951	39.9070314	93315.22663	0.173351215
	20	14.68147951	39.9070314	93315.22663	0.173351215
	20	7.376028104	40	64104.11242	0.173708047
	20	8.496423314	39.80803088	68563.61681	0.17365558
	20	11.24220574	39.8812178	79555.16301	0.173520089
	18	1.715564584	38.82029293	41326.59202	0.134000944
	20	6.386909954	39.9392454	60140.65304	0.173757292
	20	10.37615623	39.84235722	76086.49599	0.173563025
	18	5.522621313	31.88252238	55276.97533	0.07384953
	20	14.04035562	39.91208193	90751.31189	0.17338257
	20	5.121478115	39.54182695	55033.22256	0.173824438
	20	12.46624412	39.88025492	84451.20581	0.173460116
	20	13.13887464	39.59008909	87108.35881	0.173430841
	20	3.831062115	39.50073986	49866.83354	0.173888359
	20	9.843194128	39.79778345	73949.52161	0.17358971
	20	13.40097139	39.88264035	88190.38918	0.173414278
	20	9.007423858	39.75045918	70600.99824	0.17363127
	20	5.555765827	38.83334111	56688.89754	0.173812105
	20	11.86065607	40	82042.62427	0.173488272
	20	14.47402707	39.91184325	92485.97026	0.17336132
Mean	19.8	9.660946061	39.32943948	73142.66978	

APPENDIX C- LCOE Calculation

The Levelized Cost of Energy (Lcoe) is calculated from online calculator. https://www.nrel.gov/analysis/tech-lcoe

Levelized Cost of Energy Calculator	
Periods (Years):	20
Discount Rate (%):	6 (Industry Standard)
Capital Cost ($):	30500
Capital Cost ($/kW):	0.0480
Capacity Factor (%):	58
Fixed O&M Cost ($/kW-yr):	6.053
Variable O&M Cost ($/kWh):	0.06053
Electricity Price (cents/kWh):	26.7
Cost Escalation Rate (%):	3
Levelized Cost of Utility Electricity (cents/kWh):	35.8

Capital Cost ($/kW) = (Capital Expenditure / Total Energy Generated)

= (30500 / (87*365*20))

= 0.0480

Capacity Factor = The capacity factor is the ratio of actual MWh produced to the maximum possible MWh that could be produced, typically on an annual basis.

= (Actual energy produced in year \ Maximum possible energy that could be be produced) * 100%

= ((87*365 KW) / (150*365 KW)) * 100%

= 58 %

Fixed O&M Cost ($/kW-yr) = (Battery renewal every 3 years + wind turbines and electronics replaced every 10 year)

= ((40*115*7)+(2*20*4000) / (87*365))

= 6.053

Variable O&M Cost ($/kW-yr) = 0.01 * 6.053

= 0.06053

Levelized Cost of Energy (Lcoe) is calculated from online calculator.
https://www.nrel.gov/analysis/tech-lcoe = **35.8 cents/kWh**

Asmit Gautam

Final repost asmit gautam.docx

Tribhuvan University

Document Details

Submission ID

trn:oid:::3117:605029827

Submission Date

Jul 6, 2026, 11:04 AM GMT+5:45

Download Date

Jul 6, 2026, 11:07 AM GMT+5:45

File Name

Final repost asmit gautam.docx

File Size

1.6 MB

86 Pages

14,287 Words

89,194 Characters

9% Overall Similarity

The combined total of all matches, including overlapping sources, for each database.

Filtered from the Report

- Bibliography
- Quoted Text
- Cited Text
- Small Matches (less than 8 words)

Custom Section Exclusions

{titlesCount} Section Titles, {keywordsCount} Keywords

Section title	No. of Section Starters	Section Starters
"Acknowledgements"	4	Acknowledgements, Acknowledgement, Acknowledgment, Acknowledgments

Match Groups

74 Not Cited or Quoted 9%
Matches with neither in-text citation nor quotation marks

0 Missing Quotations 0%
Matches that are still very similar to source material

0 Missing Citation 0%
Matches that have quotation marks, but no in-text citation

0 Cited and Quoted 0%
Matches with in-text citation present, but no quotation marks

Top Sources

7% Internet sources
6% Publications
0% Submitted works (Student Papers)

Integrity Flags

0 Integrity Flags for Review

No suspicious text manipulations found.

Our system's algorithms look deeply at a document for any inconsistencies that would set it apart from a normal submission. If we notice something strange, we flag it for you to review.

A Flag is not necessarily an indicator of a problem. However, we'd recommend you focus your attention there for further review.

Match Groups

- **74** Not Cited or Quoted 9%
  Matches with neither in-text citation nor quotation marks
- **0** Missing Quotations 0%
  Matches that are still very similar to source material
- **0** Missing Citation 0%
  Matches that have quotation marks, but no in-text citation
- **0** Cited and Quoted 0%
  Matches with in-text citation present, but no quotation marks

Top Sources

7%	Internet sources
6%	Publications
0%	Submitted works (Student Papers)

Top Sources

The sources with the highest number of matches within the submission. Overlapping sources will not be displayed.

1	Internet	elibrary.tucl.edu.np	4%
2	Publication	Khagendra Bahadur Thapa, Arbin Maharjan, Kishor Kaphle, Kishor Joshi, Tara Ary...	<1%
3	Internet	en.wikipedia.org	<1%
4	Internet	www.frontiersin.org	<1%
5	Internet	www.mdpi.com	<1%
6	Publication	Muhammad Wakil Shahzad, Viet Hung Nguyen, Ben Bin Xu, Rasikh Tariq et al. "M...	<1%
7	Internet	publikationen.bibliothek.kit.edu	<1%
8	Internet	ir-library.ku.ac.ke	<1%
9	Publication	Riyadh Bouddou, Abdallah Belabbes, Nasreddine Bouchikhi, Ayodeji Olalekan Sal...	<1%
10	Internet	researchspace.ukzn.ac.za	<1%

11 Internet

www.researchgate.net <1%

12 Publication

Shengcan Lu, Xiangxi Han. "Multi-objective optimization of spar-type floating win... <1%

13 Internet

lis.unza.zm <1%

14 Internet

www.nepjol.info <1%

15 Publication

Asif Raza, Zi-Hong Jiang, Yi-Die Ye, Muhammad Punhal Sahto, Ahmed Lotfy Haridy... <1%

16 Publication

Ping Tang, Siew Young Quek, Aliah Zannierah Mohsin, Nurul Hanisah Juhari, Shua... <1%

17 Internet

mdpi-res.com <1%

18 Internet

ir.mu.ac.ke:8080 <1%

19 Internet

wiredspace.wits.ac.za <1%

20 Publication

Mukesh Kumar Awasthi, Sanoj Kumar, Deepika Saini. "Artificial Intelligence Tech... <1%

21 Publication

N. Nariman-zadeh, K. Atashkari, A. Jamali, A. Pilechi, X. Yao. "Inverse modelling of... <1%

22 Publication

Roque Aguado, Daniel Sánchez-Lozano, Antonio Escámez, David Vera, Francisco J... <1%

23 Internet

ebin.pub <1%

24 Internet

pure.tudelft.nl <1%

25 Publication

Habib Elkhorchani, Khaled Grayaa. "Novel home energy management system usi... <1%

26 Publication

Leonardo Azevedo Scardua. "Applied Evolutionary Algorithms for Engineers Usin... <1%

27 Publication

Mohamad Abed, Amarendra Reddy B, T.R. Jyothsna, Nabil Mohammed. "Optimal s... <1%

28 Publication

Thalita Salgado Fagundes. "Toward inclusive and sustainable water and sanitatio... <1%

29 Internet

aaltodoc.aalto.fi <1%

30 Internet

www.leadventgrp.com <1%

31 Publication

A.A. Okubanjo, Ignatius Kema Okakwu. "Optimal sizing of hybrid PV-wind-hydrog... <1%

32 Publication

Alireza Dehghani-Sanij, Mohammad Hadi Ghasemi, Andrew Wigston, Kushsairy K... <1%

33 Publication

Budhy Setiawan, Ekananda Sulistyo Putra, Indrazno Siradjuddin. "Hybrid renewa... <1%

34 Publication

Juan Pérez, Gustavo Lobos, Milena Bonacic. "Integrated forecasting and deep rei... <1%

35 Publication

K. R. Rao. "Wind Energy for Power Generation", Springer Science and Business Me... <1%

36 Publication

Kgomo, Naledi. "Incorporation of Solar Produced Power to Household Electricity ... <1%

37 Publication

Shakti Singh, Mukesh Singh, S. C. Kaushik. "A review on optimization techniques f... <1%

38 Publication

Sunanda Sinha, S.S. Chandel. "Review of recent trends in optimization techniques... <1%

39 Publication

Y. Guo, G. A. Walters, S. T. Khu, E. Keedwell. "A novel cellular automata based app... <1%

40 Internet

crses.sun.ac.za <1%

41 Internet

hdl.handle.net <1%

42 Internet

iksadyayinevi.com <1%

43 Internet

ojspanel.undikma.ac.id <1%

44 Internet

pure.strath.ac.uk <1%

45 Internet

repository.learn-portal.org <1%

46 Internet

umpir.ump.edu.my <1%

47 Internet

www.eeer.org <1%